Published in final edited form as:
Bioconjug Chem. 2013 March 20; 24(3): 473–486. doi:10.1021/bc300610f.

Trihydroxamate Siderophore-Fluoroquinolone Conjugates are Selective Sideromycin Antibiotics that Target *Staphylococcus aureus*

Timothy A. Wencewicz[a], **Timothy E. Long**[a,b], **Ute Möllmann**[c], and **Marvin J. Miller**[a,*]

[a]Department of Chemistry and Biochemistry, 251 Nieuwlan Science Hall, University of Notre Dame, Notre Dame, IN 46556, USA

[c]Leibniz Institute for Natural Product Research and Infection Biology, Hans Knöll Institute, Beutenbergstrasse 11a, 07745 Jena, Germany

Abstract

Siderophores are multidentate iron(III) chelators used by bacteria for iron assimilation. ***Sideromycins***, also called siderophore-antibiotic conjugates, are a unique subset of siderophores that enter bacterial cells via siderophore uptake pathways and deliver the toxic antibiotic in a 'Trojan Horse' fashion. Sideromycins represent a novel antibiotic delivery technology with untapped potential for developing sophisticated microbe-selective antibacterial agents that limit the emergence of bacterial resistance. The chemical synthesis of a series of mono-, bis-, and trihydroxamate sideromycins are described here along with their biological evaluation in antibacterial susceptibility assays. The linear hydroxamate siderophores used for the sideromycins in this study were derived from the ferrioxamine family and inspired by the naturally occurring salmycin sideromycins. The antibacterial agents used were a β-lactam carbacepholosporin, Lorabid®, and a fluoroquinolone, ciprofloxacin, chosen for the different locations of their biological targets, the periplasm (extracellular) and the cytoplasm (intracellular). The linear hydroxamate-based sideromycins were selectively toxic towards Gram-positive bacteria, especially *Staphylococcus aureus* SG511 (MIC = 1.0 μM for the trihydroxamate-fluoroquinolone sideromycin). Siderophore-sideromycin competition assays demonstrated that only the fluoroquinolone sideromycins required membrane transport to reach their cytoplasmic biological target and that a trihydroxamate siderophore backbone was required for protein-mediated active transport of the sideromycins into *S. aureus* cells via siderophore uptake pathways. This work represents a comprehensive study of linear hydroxamate sideromycins and teaches how to build effective hydroxamate-based sideromycins as Gram-positive selective antibiotic agents.

Introduction

Bacterial resistance to antibiotics is developing at an alarming rate.(1) As the current pipeline of useful antibacterial agents diminishes, the crisis worsens and there is now a desperate need for new methods of limiting the emergence of resistance to antibiotics. One

*To whom correspondence should be addressed. M.J.M: phone, (574) 631-7571; fax, (574) 631-6652; mmiller1@nd.edu.
[b]Current address: Department of Pharmaceutical and Biomedical Sciences, University of Georgia, Athens, GA 30602, USA

Supporting Information

List of strains, markers, and origins for microorganisms used in this work (Table S1). Tabulated biological data collected during this study (Tables S2–S3). Experimental procedures for the syntheses of compounds **1a-c, 2a-c**, and **11–14**. Copies of ^{1}H-NMR and ^{13}C-NMR spectra for compounds **1a-c, 2a-c, 3a-c**, and **11–16**. This material is available free of charge via the Internet at http://pubs.acs.org.

The authors declare no competing financial interest.

promising approach involves the development of more sophisticated, pathogen-targeted antibiotic delivery technologies that bypass or limit exposure of the antibacterial agent to known resistance mechanisms. This approach is attractive because it does not require the discovery of new antibacterial scaffolds or validation of new biological targets, which has proven to be an extremely difficult and time consuming task.(2–3) New antibiotic delivery methodologies present the opportunity to recycle old antibiotics rendered useless by resistance that have already been structurally optimized to interact with their biological target, revisit potent antibiotics abandoned due to toxicity associated with the existence of human orthologs to the biological target,(4) bring new life to antibiotic scaffolds that failed due to membrane permeability problems,(5–6) and extend the useful clinical lifetime of new antibiotics coming to market by better managing resistance.(7) Considering the serious financial investment associated with bringing a new drug to market and the limited market lifetime of antibiotics, investing in drug delivery technology is a prudent choice for antibiotic discovery programs.(8

One of the biggest challenges for targeted antibiotic delivery is finding useful biological pathways in bacteria to exploit for membrane transport.(9) The ideal membrane transport pathway for antibiotic delivery should be specific to bacterial cells (to eliminate toxicity towards eukaryotic cells), essential for virulence (to eliminate resistance development via deletion of uptake pathway), and general enough to accept unnatural substrates (to ensure successful uptake of the delivery vector derivatized to carry the antibiotic). Bacterial iron-acquisition pathways have been identified as suitable pathways for developing such antibiotic delivery systems.(10–12)

The most common pathway for bacterial iron acquisition involves the biosynthesis and excretion of low molecular weight multidentate iron(III)-chelators, known as ***siderophores***, used for extracellular solubilization of otherwise insoluble iron(III) minerals followed by proteinmediated active transport of the metal complexes into bacterial cells (Figure 1).(13–15) To ensure a competitive growth advantage, bacteria commonly possess the ability to obtain iron(III) using siderophores produced by competing organisms.(16) Along this evolutionary path, some bacteria have learned to exploit this “iron thievery” for antibiotic delivery by covalently attaching a toxic antibacterial agent to the siderophore. This unique subset of siderophores, known as ***sideromycins*** (Figure 2a), enter competing bacterial cells via siderophore uptake pathways (Figure 2b) and deliver the toxic agent in a ‘Trojan Horse’ fashion.(17

The albomycins and salmycins (Figure 2a) are two naturally occurring classes of sideromycins. The albomycins are the best studied of all sideromycins.(17) They were originally reported in 1947 from a variety of *Streptomyces* strains(18) and the structure was correctly elucidated in 1982.(19) The albomycins consist of a ferrichrome-like trihydroxamate siderophore joined through an amide bond to a thioribosyl pyrimidine inhibitor of seryl-*t*-RNA synthetase and display *in vitro* and *in vivo* broad-spectrum antibacterial activity against Grampositive and Gram-negative bacteria with extremely potent minimum inhibitory concentrations (MIC) as low as 5 ng/μL.(17) This impressive potency is attributed to active transport into bacteria via the ferrichrome membrane transport proteins FhuA(20) and FhuD.(21) Once internalized the seryl-*t*-RNA synthetase inhibitor is released by a serine protease, peptidase N, which cleaves the amide bond linkage to the siderophore.(22) The albomycins are highly effective in mouse infection models(17) and recently the biosynthetic gene cluster was discovered which makes possible the production of novel analogs and engineering of superproducers.(23)

Far less is known about the salmycins which were isolated from *Streptomyces violaceus* DSM 8286 in 1995 by Vertesy and coworkers.(24) A total synthesis of the salmycins was

completed by Miller and coworkers in 2002 which corrected the structure assignment.(25) The salmycins consist of a linear trihydroxamate siderophore from the ferrioxamine family, known as danoxamine, and an aminoglycoside antibiotic joined through a succinoyl linker (Figure 3). They show potent and selective *in vitro* antibacterial activity against Gram-positive bacteria, including highly antibiotic resistant strains, with reported MIC values as low as 10 ng/μL.(17) Similar to the albomycins, the incredible potency is attributed to active transport of the salmycins through hydroxamate siderophore membrane transport proteins.(26) Unfortunately the salmycins only show weak *in vivo* activity in mouse infection models probably due to extracellular hydrolysis of the labile ester linkage.(17) We hypothesized that intracellular hydrolysis of the aminoglycoside antibiotic was required for activity and that the ferrioxamine siderophore was responsible for the narrow spectrum of antibacterial activity against Grampositive bacteria.(27

In this report, we set out to better understand the selective antibiotic activity of the salmycins using a series of synthetic mono-, bis-, and trihydroxamate sideromycins (Figure 3) and exploit this knowledge for building more effective synthetic sideromycins. Using broad spectrum antibiotics with different biological targets, β-lactams and fluoroquinolones, we demonstrate that the full trihydroxamate siderophore backbone is required for active membrane transport and that this type of delivery vector is selective for Gram-positive bacteria that possess hydroxamate siderophore transport proteins, as reported for the salmycins and observed here against *S. aureus*. We also establish that sideromycins with intracellular antibiotic targets, which require membrane transport to be reached, should be used to target Gram-positive pathogens.

Results and Discussion

Syntheses of Siderophores and Sideromycins

The synthetic sideromycins used in this study were rationally designed to mimic the structure of the naturally occurring salmycins (Figure 3). The linear hydroxamate siderophores (**1a–3a**) were all derived from the natural siderophore portion of the salmycins containing a succinoyl linker. Sideromycins **1b–3b** featured the broad-spectrum β-lactam carbacephalosporin antibiotic Lorabid® which has a periplasmic biological target. Sideromycins **1c–3c** featured the broad-spectrum fluoroquinolone antibiotic ciprofloxacin which has a cytoplasmic biological target (Figure 4).(28

The hydroxamate siderophores and sideromycins were synthesized using a benzyl-protecting group strategy. The *bis*-*O*-benzyl (**4**), *tris*-*O*-benzyl (**5**), and *tetra*-*O*-benzyl (**6**) protected siderophore precursors were synthesized using a literature protocol developed by Roosenberg and Miller.(29) The corresponding deprotected, iron-free siderophores (**1a, 2a**, and **3a**) were prepared and isolated in high yield and purity using Pd-catalyzed hydrogenolysis followed by precipitation from MeOH/Et_2O. The iron(III)-complexed siderophore, danoxamine (**3a-Fe**), was isolated in quantitative yield as an orange solid after treatment of desferridanoxamine (**3a**) with $Fe(acac)_3$ and precipitation from MeOH/Et_2O (Scheme 1).(30)

Antibiotic derivatives **8** and **10** were synthesized for use as coupling partners with the *O*benzyl protected siderophores **4, 5**, and **6**. *N*-Boc-*O*-PNB-Lorabid® (**7**; a gift from Eli Lilly and Co.) was treated with anhydrous TFA to give TFA salt **8**. Ciprofloxacin (**9**) was converted to *O*-benzyl-ciprofloxacin HCl salt (**10**) by sequential *N*-Boc protection, carboxylate benzylation, and *N*-Boc deprotection according to a literature protocol (Scheme 2).(31) The free amines of the protected β-lactam and fluoroquinolone antibiotics, **8** and **10**, were poised for conjugation to the succinoyl group of benzyl-protected siderophore precursors **4–6** through amide bond formations. Importantly, β-lactam(32) and

fluoroquinolone(33) antibiotics are known to tolerate bulky substituents at these points of derivatization and representative siderophore-conjugates of these classes of antibiotics have been shown to retain affinity for their distinct biological targets.(34–35)

The fully protected sideromycins (**11–16**) were assembled using EDC-mediated amide couplings between the free succinoyl carboxylate of the protected siderophores (**4–6**) and the antibiotic amine salts (**8** and **10**) under basic conditions (Scheme 3). The protected Lorabid® sideromycins (**11, 13**, and **15**) were universally deprotected using hydrogenolysis conditions optimized to preserve the vinyl chloride functionality of the β-lactam bicycle.(36–39) Purification by preparative HPLC and recrystallization from MeOH/Et_2O provided analytically pure samples of the β-lactam sideromycins (**1b, 2b**, and **3b**). The *O*-benzyl protected ciprofloxacin sideromycins (**12, 14**, and **16**) were universally deprotected by Pd-catalyzed hydrogenolysis and the fluoroquinolone sideromycins (**1c, 2c**, and **3c**) were obtained in pure form after recrystallization from MeOH/Et_2O with no need for chromatographic purification.

Antibacterial Activity of Siderophores and Sideromycins Against ESKAPEE Pathogens

The siderophores, sideromycins, and control antibiotics (Lorabid® and ciprofloxacin) were tested for antibacterial activity against a panel of *ESKAPEE* bacteria (*E. faecium, S. aureus, K. pneumonia, A. baumannii, P. aeruginosa, E. aerogenes, E. coli*)(1) by determining the minimum inhibitory concentrations (MIC) using the broth microdilution assay (Table 1).(40) As expected, the siderophores (**1a–3a** and **3a-Fe**) had no antibacterial activity (MIC values >128 μM) since these molecules should be growth promoting factors. The β-lactam-hydroxamate conjugates (**1b–3b**) had moderate activity against *S. aureus* (MIC values from 32–64 μM), but at a reduced potency relative to the parent antibiotic, Lorabid® (MIC value of 1 μM). Conjugates **1b–3b** also had moderate activity against *A. baumannii* (MIC values from 32–128 μM) while Lorabid® had no measureable activity (MIC value of >128 μM). Overall the β-lactamhydroxamate conjugates (**1b–3b**) had a narrowed spectrum of activity and reduced potency (higher MIC values) against the *ESKAPEE* bacteria relative to Lorabid® alone.

The fluoroquinolone-hydroxamate conjugates (**1c–3c**) also showed a reduced spectrum of activity relative to the broadly active parent antibiotic, ciprofloxacin (Table 1). The monohydroxamate conjugate **1c** had activity against *S. aureus* (32 μM), *K. pneumonia* (16 μM), *A. baumannii* (16 μM), *P. aeruginosa* (128 μM), *E. aerogenes* (4 μM), and *E. coli* (2 μM), but at significantly reduced potencies relative to ciprofloxacin (MIC values of 0.5, 0.25, 0.25, 0.125, <0.015, and <0.015 μM, respectively). The bishydroxamate conjugate **2c** had similar activity as **1c** against *S. aureus* (64 μM), *K. pneumonia* (128 μM), *A. baumannii* (64 μM), *P. aeruginosa* (64 vM), *E. aerogenes* (4 μM), and *E. coli* (2 μM), but again at significantly reduced potencies compared to ciprofloxacin. Trihydroxamate conjugate **3c** showed selective antibacterial activity towards *S. aureus* (MIC value of 1 μM) at approximately equivalent potency as ciprofloxacin (MIC value of 0.5 μM). Mono- and bishydroxamate conjugates, **1c** and **2c**, had spectra of antibacterial activity similar to that of ciprofloxacin (broad spectrum with increased potency towards Gram-negative bacteria) at a reduced potency while the trihydroxamate conjugate **3c** had a narrow spectrum of activity primarily against Gram-positive bacteria, especially *S. aureus*.

Effect of Fe(III) Concentration on Sideromycin Antibacterial Activity

Since the hydroxamate-antibiotic conjugates (**1b–3b** and **1c–3c**) all had activity towards *S. aureus* SG511, this organism was chosen for further experiments to determine if the synthetic sideromycins were actively transported into the bacterial cells via siderophore uptake pathways. Siderophore transport pathways are known to be upregulated during times

of Fe(III)-restriction(41) and consequently it has been discovered that the potency of antibacterial activity of a sideromycin increases (lower MIC value) under these circumstances.(42) As shown in Table 2, MIC values against *S. aureus* were determined for all the conjugates using Fe(III)-supplemented (MHII + Fe) and Fe(III)-restricted (MHII − Fe) testing media.(43) None of the MIC values observed for the β-lactam-hydroxamate conjugates (**1b–3b**) under varying Fe(III) concentrations changed significantly (a significant change for the broth microdilution assay is >2-fold). Only trihydroxamate conjugate **3c** produced a significant (4–fold) decrease in MIC value when going from Fe(III)-supplemented media (4 μM) to Fe(III)-restricted media (1 μM). The MIC values for the control antibiotics, Lorabid® and ciprofloxacin, showed no dependence on the Fe(III) concentration. These data suggest that the fluoroquinolone-trihydroxamate conjugate **3c** might be utilizing siderophore-transport pathways.

Effect of Competing Siderophores on Sideromycin Antibacterial Activity

Sideromycin antibacterial activity is known to be antagonized in the presence of siderophores competing for uptake via the same membrane transport systems.(44) To screen for this type of antagonism, MIC values against *S. aureus* were determined under Fe(III)-restricted conditions using 1:1 molar mixtures of the hydroxamate-antibiotic conjugates (**1b–3b** and **1c–3c**) with the corresponding parent hydroxamate compounds (**1a–3a** and **3a-Fe**) and the commercially available trihydroxamate siderophore desferrioxamine B (**DFO-B**) or its Fe(III) complex ferrioxamine B (**FO-B**), as shown in Table 3. The siderophore **DFO-B** and siderophore-Fe(III) complex **FO-B** were chosen since they are known to be utilized by *S. aureus* for siderophore-mediated Fe(III)-acquisition and are structurally similar to danoxamine, the siderophore portion of the salmycins.(45) The antibacterial activity of the β-lactam-monohydroxamate conjugate **1b** was not antagonized by the monohydroxamate **1a** (Table 3, Entry 1) or **DFO-B** (Table 3, Entry 2). The activity of the β-lactam-bishydroxamate conjugate **2b** was not antagonized, but was enhanced by the presence of bishydroxamate **2a** (Table 3, Entry 3) or **DFO-B** (Table 3, Entry 4). Similarly, the activity of the β-lactam-trihydroxamate conjugate **3b** was not antagonized by the presence of trihydroxamate-Fe(III) complex **3a-Fe** (Table 3, Entry 6) or **FO-B** (Table 3, Entry 8) and was slightly enhanced by the trihydroxamate **3a** (Table 3, Entry 5) and **DFO-B** (Table 3, Entry 7).

Neither the mono- or bishydroxamate-fluoroquinolone conjugates **1c** and **2c**, respectively, were antagonized by the presence of the parent hydroxamate compounds (**1a** and **2a**, respectively) or **DFO-B** (Table 3, Entries 9–12). The fluoroquinolone-trihydroxamate conjugate **1c** was not antagonized by the parent trihydroxamate siderophore **3a** (Table 3, Entry 13) or the Fe(III)-complex **3a-Fe** (Table 3, Entry 14). However, conjugate **3c** was strongly antagonized by the trihydroxamate siderophore **DFO-B** (Table 3, Entry 15) and the Fe(III)-complex **FO-B** up to >128-fold. Antagonism of the antibacterial activity of **3c** by **DFO-B** and **FO-B** suggests that these molecules are competing for entrance into *S. aureus* cells via siderophore-uptake pathways.

The influence of competing siderophores **3a, 3a-Fe, DFO-B**, and **FO-B** on the antibacterial activity of the β-lactam-trihydroxamate conjugate **3b** (Figure 5a,b) and the fluoroquinolone-trihydroxamate conjugate **3c** (Figure 5c,d) against *S. aureus* was also studied using a qualitative agar diffusion competition experiment (Figure 5). Sterile paper strips soaked in solutions of the test compounds were layed in a ‘cris-cross’ pattern on Fe(III)-deficient MHII agar inoculated with *S. aureus*. After incubation and growth of the organism, analysis of the intersecting and nonintersecting points of the paper strips revealed the effects of the compound mixtures relative to the single compounds alone. Data from these studies was in agreement with the data from the MIC studies (Table 3). The antibacterial activity of the β-

lactamtrihydroxamate conjugate **3b** was not antagonized by the presence of **3a-Fe** and **FO-B** and was slightly enhanced by the presence of **3a** and **DFO-B** while the activity of Lorabid® was unaffected (Figure 5a,b). The antibacterial activity of the fluoroquinolone-trihydroxamate conjugate **3c** was antagonized by all the siderophores (**3a, 3a-Fe, DFO-B**, and **FO-B**) while ciprofloxacin was unaffected. In agreement with the MIC data (Table 3), **DFO-B** and **FO-B** antagonized the activity of **3c** more than siderophores **3a** and **3a-Fe** (Figure 5c,d).

Further Sideromycin Antibacterial Susceptibility Testing in Agar Diffusion Assays

A more quantitative agar diffusion assay was used to further verify the observed affects of variable Fe(III) concentrations and competing siderophores on the anti-*S. aureus* activity of the hydroxamate-antibiotic conjugates (Figures 6 and 7). The quantitative agar diffusion assay used was a modified(46) Kirby-Bauer assay.(47) Compound solutions were added to 9 mm wells of an agar petri dish inoculated with *S. aureus* SG511 according to the conditions indicated in the captions and color-coded legends of Figures 6 and 7. After incubation, the diameter of growth inhibition zones were measured and are reported on the vertical axes as the average of three independent trials. As shown in Figure 6, the antibiotic activities of the β-lactamhydroxamate conjugates **1b–3b** and Lorabid® against *S. aureus* were not significantly affected by changes in the concentration of Fe(III) in the testing media or by the presence of competing siderophores. These observations are consistent with the MIC values discussed previously (Tables 2 and 3).

As shown in Figure 7, all three of the fluoroquinolone-hydroxamate conjugates (**1c–3c**) showed decreased potency (smaller diameter zone of growth inhibition) against *S. aureus* in Fe(III)-supplemented media (MHII + Fe) relative to Fe(III)-restricted media (MHII – Fe). Furthermore, the potency of conjugates **1c–3c** all decreased in the presence of an equimolar amount of the competing parent siderophores (**1a–3a**, respectively) or **DFO-B**. Again in agreement with MIC data from Table 3, antagonism of the fluoroquinolone-trihydroxamate conjugate **3c** by **DFO-B** and **FO-B** was more pronounced than by the parent siderophore **3a** and its Fe(III)-complex **3a-Fe**. These data again strongly support that the trihydroxamate conjugate **3c** is utilizing the same siderophore-transport pathway as **DFO-B** to deliver the fluoroquinolone antibiotic to its cytoplasmic target (DNA gyrase) in *S. aureus*.

Further Discussion

The hydroxamate-β-lactam (**1b–3b**) and hydroxamate-fluoroquinolone conjugates (**1c–3c**) from this study all showed a narrowed spectrum of activity compared to the parent antibiotics. The hydroxamate-antibiotic conjugates showed high selectivity towards the Gram-positive pathogen *Staphylococcus aureus* SG511. The trihydroxamate-fluoroquinolone conjugate **3c** showed the most selective activity and retained equivalent potency as the parent antibiotic, ciprofloxacin, against *S. aureus* (MIC = 1 μM). Sideromycin **3c** represents one of the few synthetic siderophore-antibiotic conjugate using an antibiotic with an intracellular target that maintains the potency of the parent drug.(27, 35) The trihydroxamate siderophore, desferridanoxamine (**3a**), clearly was responsible for the narrowed spectrum of activity of the trihydroxamate-ciprofloxacin conjugate (**3c**). Analogously, desferridanoxamine is also the likely source of the exquisite Gram-positive selectivity observed for the salmycins which contain a normally broad spectrum aminoglycoside antibiotic. The precise reason for the selective antibacterial activity against Gram-positive bacteria is still up for debate, but one possibility is that the more promiscuous membrane-anchored hydroxamate siderophore binding proteins in *S. aureus*, known as FhuD1 and FhuD2, are capable of binding to the salmycins and the trihydroxamate-ciprofloxacin conjugate with high affinity while the more discriminative hydroxamate

siderophore outer membrane proteins found in Gram-negative bacteria have reduced affinity for the derivatized siderophores.(45, 48–49)

Antibacterial susceptibility testing in both the broth microdilution and agar diffusion assays revealed that the antibacterial activity of the hydroxamate-β-lactam conjugates (**1b–3b**) against *S. aureus* showed no dependence on Fe(III) concentration in the media and was unaffected by the presence of competing siderophores. These observations are consistent with the fact that the β-lactam biological targets, the penicillin binding proteins (PBPs), are in the periplasmic peptidoglycan which is outside of the cell membrane for *S. aureus*. Therefore, active transport into the *S. aureus* cells actually denied the β-lactam sideromycins access to *S. aureus* PBPs. The hydroxamate-fluoroquinolone conjugates required active transport across the cell membrane to reach their biological target (DNA gyrase) in the cytoplasm. This clearly demonstrated that siderophore-antibiotic conjugates targeting Gram-positive bacteria should only use antibiotics with cytoplasmic targets. Furthermore, antibacterial activity of the trihydroxamate-ciprofloxacin conjugate (**3c**) showed a significant dependence on Fe(III) concentration in the testing media and was antagonized by competing siderophores while the antibacterial activities of the mono- and bishydroxamate-ciprofloxacin conjugates (**1c** and **2c**, respectively) were less influenced by Fe(III) and competing siderophores in the testing media. This suggested that the entire trihydroxamate backbone of the siderophore is necessary to facilitate efficient active transport of the sideromycin by *S. aureus*. The likely reason for needing the full trihydroxamate siderophore is for competitive chelation of environmental Fe(III) and recognition of the siderophore-Fe(III) complex by the siderophore-binding receptor proteins, which preferentially bind to octahedral, trihydroxamate-Fe(III) complexes.(14

The ability of the ferrioxamine siderophore **DFO-B** and its Fe(III) complex **FO-B** to antagonize the anti-*S. aureus* activity of sideromycin **3c** to a much greater extent than the structurally similar trihydroxamate parent siderophore desferridanoxamine, **3a**, and its Fe(III)-complex danoxamine, **3a-Fe**, is attributed to the drastic difference in Fe(III)-affinity observed for these molecules. Desferrioxamine B has an Fe(III)-affinity ($\sim 10^{30}$) which is ~7 orders of magnitude greater than the Fe(III)-affinity of trihydroxamate siderophore **3a** ($\sim 10^{23}$) (unpublished data from our laboratory). In so far unpublished work, we have shown that a competing siderophore must have an Fe(III)-affinity equal to or greater than the sideromycin in order to antagonize the antibacterial activity of the sideromycin. This observation is attributed to the fact that the sideromycin can only be transported into bacterial cells as the Fe(III)-complex and the molecule with the higher Fe(III)-affinity will ‘win’ the competition for entry into the bacterial cell by ‘winning’ the competition for binding the scarce Fe(III) nutrient.

Since a stable amide bond linkage was formed between the antibiotic ciprofloxacin and the siderophore desferridanoxamine, it was suspected that the entire desferridanoxamine-ciprofloxacin was the active antibacterial agent inhibiting the action of DNA gyrase. This hypothesis is supported in the literature by examples of siderophore-ciprofloxacin conjugates linked through an amide bond on the distal nitrogen of the piperazine unit that still show high *in vitro* binding to DNA gyrase.(35) The question of whether or not the aminoglycoside antibiotic of the salmycins is released inside bacterial cells is still up for debate, but it is proposed that the ideal synthetic sideromycin should feature a microbe-triggered linker that releases the antibiotic inside the cell to give optimal affinity for the biological target.(27) In fact, the development of new linker systems that make such intracellular release possible have been the focus of much work in our group.(50

The trihydroxamate-ciprofloxacin sideromycin **3c** developed in this work has many potential applications. The exquisite selectivity against *S. aureus* makes sideromycin **3c** an ideal

candidate for a targeted microbe-selective antibacterial chemotherapy that could limit the spread of fluoroquinolone multidrug resistance by limiting exposure of nontargeted bacteria to the active ingredient. Sideromycin **3c** has the potential for decreasing mammalian toxicity of fluoroquinolones since it selectively enters *S. aureus* cells via membrane transport systems that are absent in eukaryotic cells.(51) Trihydroxamate ferrioxamine siderophores, including FDAapproved **DFO-B**, have been proven safe for human consumption at extremely large doses (4–12 g/day) when given to patients for chelation treatment of iron-overload diseases.(52) It has been documented that the use of **DFO-B** to treat iron-overload during the course of an *S. aureus* infection can worsen the infection since *S. aureus* can use the Fe(III)-complex **FO-B** for ironassimilation.(45) Using sideromycin **3c** to treat iron-overload diseases might be an effective method for simultaneously treating or preventing *S. aureus* infections. In fact, the salmycins have been patented for such an intended use.(53–54) Additionally, ferrioxamine siderophores are not bound by the mammalian siderophore-binding protein siderocalin, so the bioavailability is predicted to be high and consequently the required dosing to treat bacterial infections might be low.(55

One foreseeable limitation of sideromycin antibiotics, and most pathogen-targeted antibiotic agents, is that they might not be effective at treating intracellular infections caused by pathogenic microbes that survive inside mammalian cells since the delivery agent is not engineered to penetrate higher eukaryotic cells.(56) Fortunately, alternative methods for treating these types of infections with engineered delivery systems are in development.(57) Another potential limitation to sideromycin antibiotic chemotherapy born from their exquisite microbe-selectivity is the need for sensitive pathogen detection and rapid diagnostics. Unlike broad-spectrum antibiotics, microbe-selective antibiotics such as sideromycins will require early pathogen identification to direct accurate antibacterial drug prescription.(2) Fortunately, major advancements in bacterial pathogen detection using siderophore-based sensors are in development by several groups and will certainly play an important role in the future for progressing sideromycin antibiotics into the clinic.(58–59)

Summary and Conclusions

Similar to the salmycins, the synthetic linear hydroxamate sideromycins studied here showed selective antibacterial activity against Gram-positive bacteria, especially *Staphylococcus aureus* SG511 (MIC = 1 μM for the trihydroxamate-fluoroquinolone sideromycin **3c**). Siderophore-sideromycin competition assays and bacterial growth inhibition assays using variable Fe(III) concentrations showed that only the fluoroquinolone sideromycins (**1c–3c**) required membrane passage to reach their cytoplasmic biological target and that the full trihydroxamate siderophore delivery vector was required for siderophore-associated protein-mediated active transport into *S. aureus* cells. This work supports the hypothesis that linear trihydroxamate siderophores are selective antibiotic delivery vectors for Gram-positive pathogens, as observed for the naturally occurring salmycins and the synthetic desferridanoxamine-ciprofloxacin sideromycin (**3c**), and teaches how to engineer more effective hydroxamate-based sideromycins.

Experimental Section

Materials and Instrumentation

All reactions were performed under a dry argon atmosphere, unless otherwise stated. All solvents and reagents were obtained from commercial sources and used without further purification unless otherwise stated. Dichloromethane (CH_2Cl_2) was distilled from calcium hydride. Dimethylformamide (DMF) and diisopropylethylamine (iPr$_2$EtN) were used from Acros Seal anhydrous bottles. *N*-Boc-*O*-PNB-Lorabid® (**7**) was a gift from Eli Lilly and Company. Ciprofloxacin (**9**) was purchased from Sigma-Aldrich (St. Louis, MO). Benzyl

protected hydroxamate siderophores **4–6** were prepared according to a previously described method.(29) Silica gel column chromatography was performed using Sorbent Technologies silica gel 60 (32–63 μm).

All microbiological media and liquids were sterilized by autoclaving (121 °C, 15 min) before use unless otherwise stated. All aqueous solutions and media were prepared using distilled, deionized, and filtered water (Millipore Milli-Q Advantage A10 Water Purification System). Luria broth (LB) was purchased from VWR. Mueller-Hinton No. 2 broth (MHII broth; cation adjusted) was purchased from Sigma-Aldrich (St. Louis, MO). Iron-deficient MHII broth (MHII − Fe) was prepared by adding 0.8 mL of a 1 mg/mL filter-sterilized aqueous solution of 2,2′-bipyridine to 49.2 mL of sterile MHII broth. Iron-supplemented MHII broth (MHII + Fe) was prepared by adding 0.8 mL of a freshly prepared 1 mg/mL filter-sterilized aqueous solution of $FeCl_3$ to 49.2 mL of sterile MHII broth. Mueller-Hinton No. 2 agar (MHII agar; HiMedia Laboratories) was purchased from VWR. Iron-deficient MHII agar (MHII – Fe) was prepared by adding 0.5 mL of a 1 mg/mL filter-sterilized aqueous solution of 2,2'-biypridine to 34 mL of melted MHII agar with gentle mixing. Iron-supplemented MHII agar (MHII + Fe) was prepared by adding 0.5 mL of a freshly prepared 1 mg/mL filter-sterilized aqueous solution of $FeCl_3$ to 34 mL of melted MHII agar with gentle mixing. McFarland $BaSO_4$ turbidity standards were purchased from bioMerieux, Inc. Sterile plastic petri dishes (145 mm × 20 mm; Greiner Bio-One) and sterile polystyrene 96-well plates (BD Falcon) used for antibacterial susceptibility testing were purchased from VWR. Ferric chloride (anhydrous, reagent grade) and 2,2'-bipyridine (reagent plus grade) were purchased from Sigma-Aldrich. All test organisms used in this work were from sources given in the Supporting Information (Table S1).

^{1}H-NMR and ^{13}C-NMR spectra were obtained on a 300, 500, or 600 MHz Varian DirectDrive spectrometer and FIDs were processed using ACD/ChemSketch version 10.04. Chemical shifts (δ) are given in parts per million (ppm) and are referenced to residual solvent. Coupling constants (*J*) are reported in hertz (Hz). High resolution, accurate mass measurements were obtained with a Bruker micrOTOF II electrospray ionization time-of-flight mass spectrometer in positive ion mode. Sample was introduced via flow injection at a rate of 4 μL/min, and mass spectra were accumulated from 50–3000 m/z for two minutes. Preparative HPLC purifications were performed on a Waters preparative binary pump system at a flow rate of 15 mL/min with UV detection at 254 nm using a YMC-Pack Pro C18 column (150 × 20 mm; 5 μm particle size) fit with a guard column. Thin layer chromatography (TLC) was performed with Al-backed Merck 60-F_{254} or Al-backed Merck RP-C18 F_{256} silica gel plates using a 254 nm lamp and aqueous $FeCl_3$ for visualization. Melting points were determined in capillary tubes using a Thomas Hoover melting point apparatus and are uncorrected.

Representative Synthetic Procedures for the Synthesis of Siderophores and Sideromycins

Desferridanoxamine (3a)—Prepared as described previously.(29–30) Briefly, tetra-*O*benzyldanoxamine **6** (340.0 mg, 0.35 mmol) was dissolved in 35 mL MeOH in an HCl-washed round bottom flask sealed under argon. The flask was charged with 10% Pd-C (50.0 mg) and exposed to a balloon of hydrogen gas (~1 atm). Reaction progress was monitored by RP-C18 TLC (1.5:1 CH_3CN:H_2O; $FeCl_3$ stain) and after 11 h there was no remaining starting material (**6**). The flask was flushed with argon and the mixture was diluted with warm MeOH, vacuum filtered through a pad of celite using a fine glass frit, and concentrated under reduced pressure. The resulting solid was dissolved in a minimal amount of MeOH and precipitated by addition of cold Et_2O. After trituration with Et_2O, the siderophore desferridanoxamine (**3a**) was obtained in 97% yield as a white solid (208.0 mg, 0.34 mmol). Mp 134–140 °C; ^{1}H-NMR (600 MHz, DMSO-d_6) δ 11.87 (br s, COOH, 1 H),

9.62 (br s, N-OH, 3 H), 7.78 (t, J = 5.3 Hz, 2 H), 4.35 (br s, 1 H), 3.47.3.42 (m, 6 H), 3.39–3.36 (m, 2 H), 3.02–2.97 (m, 4 H), 2.57 (t, J = 6.6 Hz, 6 H), 2.39 (t, J = 6.6 Hz, 2 H), 2.26 (t, J = 6.9 Hz, 4 H), 1.49 (dt, J = 14.2, 7.1 Hz, 6 H), 1.43–1.34 (m, 6 H), 1.27–1.17 (m, 6 H); ^{13}C-NMR (150 MHz, DMSO-d_6) δ 174.1, 172.0, 171.9, 171.6, 171.3, 60.6, 47.2, 47.1, 38.4, 32.2, 29.9, 28.8, 28.7, 27.6, 27.5, 27.1, 26.2, 26.0, 23.5, 23.4, 22.7; HRMS-ESI (m/z): $[M+H]^+$ calcd. for $C_{27}H_{50}N_5O_{11}$: 620.3501, found 620.3506.

Danoxamine (3a-Fe)—Prepared as described previously.(29–30) Briefly, siderophore **3a** (154 mg, 0.25 mmol) was dissolved in 10 mL of MeOH at 40 °C (oil bath temperature). $Fe(acac)_3$ (97.0 mg, 0.28 mmol) was added and the clear, orange solution was stirred for 2 h. The solution was cooled to rt and the MeOH was evaporated under reduced pressure. The resulting orange residue was dissolved in a minimal amount of MeOH and precipitated by addition of cold Et_2O. After trituration with Et_2O, the Fe(III)-complexed siderophore danoxamine (**3a-Fe**) was isolated in 99% yield as an orange powder (165.2 mg, 0.25 mmol). Mp 151–154 °C (dec.); HRMS-ESI (m/z): $[M+H]^+$ calcd. for $C_{27}H_{47}FeN_5O_{11}$: 673.2616, found 673.2647.

O*-PNB-Lorabid® TFA salt (8)—N*-Boc-*O*-PNB-Lorabid® (**7**; 208.0 mg, 0.36 mmol) was dissolved in 7 mL of anhydrous TFA:CH_2Cl_2 (1:1). After 30 min, TLC (2:1 hexanes:EtOAc) showed complete consumption of the starting material. The TFA/CH_2Cl_2 were removed by evaporation under reduced pressure giving TFA salt **8** as a light yellow viscous oil (208.0 mg, 0.36 mmol) that was used immediately in the next reaction without purification or characterization.

***O*-Benzyl-ciprofloxacin HCl salt (10—**Prepared by a modified literature procedure.(31) Ciprofloxacin (**9**; 1.01 g, 3.05 mmol), Boc anhydride (820.0 mg, 3.76 mmol), and $NaHCO_3$ (1.28 g, 15.24 mmol) were suspended in 25 mL of anhydrous DMF and stirred at rt for 2 h. Benzyl bromide (1.62 mL, 13.64 mL) was added and the mixture was heated to 90 °C (oil bath temperature). After 1 h of heating, the reaction mixture became homogeneous. After 25.5 h of heating, the mixture was cooled to rt and the DMF was removed using high vacuum rotary evaporation (~1 mm Hg). The resulting solid was dissolved in 75 mL of $CHCl_3$ and 50 mL of H_2O. The layers were separated and the $CHCl_3$ was washed with H_2O (25 mL) and brine (25 mL), dried over anhydrous $MgSO_4$, filtered, and concentrated to give an orange solid. The crude solid was suspended in Et_2O, filtered, and washed several times with Et_2O. This provided *N*Boc-*O*-benzyl-ciprofloxacin in 98% yield as a pale yellow solid (1.56 g, 2.99 mmol). Mp 191–193 °C; ^{1}H-NMR (600 MHz, $CDCl_3$) δ 8.52 (s, 1 H), 8.05 (d, J = 13.5 Hz, 1 H), 7.52 (d, J = 7.0 Hz, 2 H), 7.38 (t, J = 7.5 Hz, 2 H), 7.33–7.29 (m, 1 H), 7.26 (d, J = 7.0 Hz, 1 H), 5.39 (s, 2 H), 3.69–3.62 (m, 4 H), 3.44–3.37 (m, 1 H), 3.24–3.19 (m, 4 H), 1.50 (s, 9 H), 1.32–1.27 (m, 2 H), 1.15–1.09 (m, 2 H); ^{13}C-NMR (150 MHz, $CDCl_3$) δ 173.0, 165.5, 154.6, 153.3 (d, $J_{C\text{-}F}$= 248.5 Hz), 148.3, 144.4 (d, $J_{C\text{-}F}$= 10.1 Hz), 137.9, 136.4, 133.3, 129.3, 128.5, 127.9, 127.8, 123.3 (d, $J_{C\text{-}F}$= 6.2 Hz), 113.4 (d, $J_{C\text{-}F}$= 24.1 Hz), 110.2, 105.0, 80.2, 66.3, 49.9, 34.5, 28.4, 8.1; HRMS-ESI (m/z): $[M+H]^+$ calcd. for $C_{29}H_{33}FN_3O_5$: 522.2399, found 522.2423. The solid (1.50 g, 2.88 mmol) was dissolved in 25 mL of CH_2Cl_2 and concentrated HCl (5 mL) was added slowly giving a dark orange solution. After 40 min, the CH_2Cl_2/HCl were evaporated giving a yellow solid. The solid was dissolved in hot MeOH (25 mL), activated charcoal was added, and the mixture was vacuum filtered through celite. The MeOH was evaporated and the solid was recrystallized from CH_2Cl_2/Et_2O at −20 °C which gave the desired *O*-benzyl-ciprofloxacin monohydrochloride salt (**10**) in 92% as a yellow solid (1.20 g, 2.62 mmol). Mp 250–255 °C (dec.); ^{1}H-NMR (600 MHz, DMSO-d_6) δ 9.71 (br s, 1 H), 9.62 (br s, 1 H), 8.48 (d, J = 3.5 Hz, 1 H), 7.84–7.77 (m, 1 H), 7.51–7.44 (m, 3 H), 7.42–7.36 (m, 2 H), 7.32 (t, J = 7.0 Hz, 1 H), 5.27 (s, 2 H), 3.65–3.53 (m, 1 H), 3.53–3.46 (m, 4 H), 3.34–3.24 (m, 4 H), 1.28–1.23 (m,

2 H), 1.12–1.07 (m, 2 H); ^{13}CNMR (150 MHz, DMSO-d_6) δ 171.6, 164.5, 152.4 (d, $J_{C\text{-}F}$= 246.8 Hz), 148.6, 142.8 (d, $J_{C\text{-}F}$= 10.7 Hz), 138.0, 136.6, 128.4, 127.7, 127.6, 122.5, 111.8 (d, $J_{C\text{-}F}$= 24.1 Hz), 108.9, 106.7, 65.2, 46.4, 42.5, 34.9, 7.6; HRMS-ESI (m/z): $[M+H]^+$ calcd. for $C_{24}H_{25}FN_3O_3$: 422.1874, found 422.1871.

tetra-*O*-Benzyldanoxamine-*O*-PNB-Lorabid® conjugate (15)—*O*-PNB-Lorabid® TFA salt (**8**; 85.7 mg, 0.15 mmol) was dissolved in 10 mL of anhydrous CH_2Cl_2 and *i*Pr_2EtN (0.13 mL, 0.75 mmol) was added slowly until the solution was basic (pH paper). tetra-*O*-Benzyl-trihydroxamate **6** (155.5 mg, 0.16 mmol), DMAP (8.0 mg, 0.06 mmol), and EDC-HCl (95.0 mg, 0.50 mmol) were then added, respectively. After 20 h at rt, TLC (3% MeOH in EtOAc; $FeCl_3$ stain) showed no remaining starting material (**8**). The CH_2Cl_2 was removed under reduced pressure and the resulting oil was dissolved in EtOAc (20 mL), washed with 1 N HCl_{aq} (15 mL), H_2O (10 mL), 10% aqueous $NaHCO_3$ (10 mL), and brine (10 mL), dried over anhydrous $MgSO_4$, filtered, and concentrated. The crude product was purified by silica gel column chromatography (1 × 6 in silica gel; 3%.5% MeOH in EtOAc) to give the desired product (**15**) in 87% yield as a clear, colorless oil (183.0 mg, 0.100.13 mmol). ^{1}H-NMR (500 MHz, $CDCl_3$) δ 8.61 (d, *J* = 7.4 Hz, 1 H), 8.21 (d, *J* = 8.6 Hz, 2 H), 7.60 (d, *J* = 8.8 Hz, 2 H), 7.45–7.24 (m, 25 H), 6.75 (br s, 1 H), 6.45 (br s, 1 H), 5.65 (d, *J* = 7.0 Hz, 1 H), 5.46 - 5.42 (m, 1 H), 5.41 (d, *J* = 14.4 Hz, 1 H), 5.33. 5.28 (m, 1 H), 4.86–4.77 (m, 5 H), 4.75 (d, *J* = 10.2 Hz, 1 H), 4.47 (s, 2 H), 4.03–3.93 (m, 1 H), 3.91–3.85 (m, 1 H), 3.66–3.56 (m, 2 H), 3.52–3.46 (m, 1 H), 3.46–3.37 (m, 3 H), 3.34–3.10 (m, 4 H), 3.00–2.92 (m, 1 H), 2.87–2.71 (m, 6 H), 2.65–2.50 (m, 5 H), 2.51–2.41 (m, 4 H), 1.68–1.55 (m, 6 H), 1.55–1.46 (m, 2 H), 1.46–1.39 (m, 3 H), 1.39–1.30 (m, 4 H), 1.24–1.16 (m, 4 H), 1.15–1.06 (m, 1 H); ^{13}C-NMR (125 MHz, $CDCl_3$) δ 174.3, 174.2, 173.8, 172.4, 172.2, 171.9, 171.4, 165.2, 160.0, 147.8, 142.1, 138.5, 136.9, 134.4, 134.2, 134.1, 130.8, 129.2, 129.1, 129.1, 129.1, 129.1, 129.0, 128.9, 128.8, 128.8, 128.7, 128.7, 128.7, 128.6, 128.6, 128.5, 128.3, 128.2, 127.7, 127.5, 127.4, 123.9, 123.7, 123.6, 123.1, 77.2, 76.3, 76.1, 72.8, 70.1, 66.2, 58.8, 57.6, 52.8, 45.5, 44.8, 43.7, 39.3, 39.2, 31.9, 30.6, 30.3, 30.1, 29.6, 29.3, 28.8, 28.1, 27.8, 27.7, 27.5, 26.7, 26.2, 25.7, 23.7, 23.4, 23.3, 21.3; HRMS-ESI (m/z): $[M+H]^+$ calcd. for $C_{78}H_{93}ClN_9O_{16}$: 1446.6423, found 1446.6416.

Desferridanoxamine-Lorabid® conjugate (3b)—tetra-*O*-Benzyl-trihydroxamate-Lorabid® conjugate **15** (110.2 mg, 0.08 mmol) and concentrated HCl (33.0 μL, 24.0 mmol) were dissolved in 1.1 mL of DMF:H_2O (95:5) in an HCl-washed, 10 mL round bottom flask sealed under argon. The flask was charged with 10% Pd-C (23.0 mg) and exposed to a balloon of hydrogen gas (~1 atm). Reaction progress was monitored by RP-C18 TLC (2.5:1 H_2O:CH_3CN; $FeCl_3$ stain) and after 24 h there was no remaining starting material (**15**). The flask was flushed with argon and the mixture was diluted with MeOH, vacuum filtered through celite, and concentrated using high vaccum rotary evaporation (~1 mm Hg). The crude product was sequentially purified by size exclusion chromatography (0.5 × 6 in Sephadex G50; 1:1 MeOH:EtOAc eluent), preparative HPLC using a 150 × 20 mm YMC-Pack Proc C18 column fit with a guard column, 0.1% TFA in H_2O (A) and 0.1% TFA in CH_3CN (B) as mobile phases, and a flow rate of 15 mL/min. A gradient was formed from 20%–50% of B over 4 min where the desired compound (**3b**) eluted at 4.1 min. Pure fractions were lyophilized and the obtained solid was recrystallized from MeOH/Et_2O to give the desired product (**3b**) in 42% yield as an off-white solid (30.0 mg, 0.03 mmol). Mp 103–105 ° (color change), 170–175 °C (dec.); ^{1}H-NMR (600 MHz, CD_3OD) δ 7.45. 7.32 (m, 5 H), 5.43.5.42 (m, 1 H), 5.37 (d, *J* = 5.0 Hz, 1 H), 3.88 (td, *J* = 7.9, 3.8 Hz, 1 H), 3.83 (ddd, *J* = 14.0, 7.3, 7.1 Hz, 1 H), 3.62–3.53 (m, 4 H), 3.30–3.26 (m, 1 H), 3.18–3.13 (m, 4 H), 2.84 (t, *J* = 6.3 Hz, 2 H), 2.76 (td, *J* = 7.1, 3.1 Hz, 3 H), 2.70–2.54 (m, 5 H), 2.53 (d, *J* = 5.6 Hz, 1 H), 2.50–2.43 (m, 4 H), 2.40 (dt, *J* = 15.2, 5.5 Hz, 1 H), 1.78–1.72 (m, 2 H), 1.68–1.57 (m, 6 H), 1.57–1.54 (m, 2 H), 1.54–1.47 (m, 4 H), 1.39–1.35 (m, 2 H), 1.34–1.27 (m, 4

H); ^{13}C-NMR (150 MHz, CD_3OD) δ 175.6, 175.1, 174.6, 174.6, 174.6, 174.5, 173.9, 166.3, 163.9, 138.3, 130.0, 129.7, 129.4, 129.1, 126.0, 62.9, 59.9, 59.6, 54.1, 40.5, 40.4, 33.4, 32.5, 31.7, 31.6, 31.3, 30.5, 30.2, 30.1, 30.0, 29.9, 29.1, 29.0, 28.9, 27.6, 27.4, 27.2, 25.0, 24.8, 24.1, 23.1; HRMS-ESI (m/z): $[M+H]^+$ calcd. for $C_{43}H_{64}ClN_8O_{14}$: 951.4225, found 951.4234.

tetra-*O*-Benzyldanoxamine-*O*-benzylciprofloxacin conjugate (16)—*O*-Benzyl-ciprofloxacin hydrochloride salt (**10**) was free-based using Amberlite IR400(OH^-) resin in $CHCl_3$ for 4 h. The resulting *O*-benzyl-ciprofloxacin amine (46.0 mg, 0.11 mmol), tetra-*O*-Benzyl-trihydroxamate **6** (103.0 mg, 0.10 mmol), *i*Pr_2EtN (0.04 mL, 0.23 mmol), DMAP (3.2 mg, 0.03 mmol), and EDC-HCl (30.2 mg, 0.16 mmol) were dissolved in 10 mL of anhydrous CH_2Cl_2, respectively. After 4.5 h at rt, TLC (9% MeOH in CH_2Cl_2; $FeCl_3$ stain) showed no remaining starting material **6**. The mixture was diluted with CH_2Cl_2 (20 mL), washed with 10% aqueous citric acid (15 mL), H_2O (15 mL), 10% aqueous $NaHCO_3$ (15 mL), and brine (15 mL), dried over anhydrous $MgSO_4$, filtered, and concentrated. The crude product was purified by silica gel column chromatography (1 × 4 in silica gel; 3% MeOH in CH_2Cl_2) to give the desired product (**16**) in 84% yield as a clear, yellow oil (121.5 mg, 0.09 mmol). ^{1}H-NMR (600 MHz, $CDCl_3$) δ 8.53 (s, 1 H), 8.07 (d, *J* = 12.9 Hz, 1 H), 7.52 (d, *J* = 7.3 Hz, 2 H), 7.43–7.24 (m, 24 H), 6.46 (br s, 1 H), 6.33 (br s, 1 H), 5.39 (s, 2 H), 4.91 (s, 2 H), 4.84 (s, 4 H), 4.47 (s, 2 H), 3.86–3.82 (m, 2 H), 3.76–3.73 (m, 2 H), 3.69–3.58 (m, 6 H), 3.44 (t, *J* = 6.6 Hz, 2 H), 3.42–3.37 (m, 1 H), 3.31–3.27 (m, 2 H), 3.24–3.16 (m, 6 H), 2.86–2.76 (m, 6 H), 2.70 (t, *J* = 6.0 Hz, 2 H), 2.47 (t, *J* = 6.2 Hz, 4 H), 1.68–1.58 (m, 8 H), 1.52–1.45 (m, 4 H), 1.42–1.24 (m, 8 H), 1.12–1.08 (m, 2 H); ^{13}C-NMR (150 MHz, $CDCl_3$) δ 174.0, 173.8, 173.7, 173.0, 172.9, 172.1, 172.0, 170.4, 165.5, 153.3 (d, $J_{C\text{-}F}$ = 249.1 Hz), 148.3, 144.1 (d, $J_{C\text{-}F}$ = 10.7 Hz), 138.5, 137.9, 136.4, 134.5, 134.3, 129.1, 129.0, 128.9, 128.8, 128.8, 128.6, 128.5, 128.3, 127.9, 127.8, 127.5, 127.4, 123.5 (d, $J_{C\text{-}F}$ = 6.7 Hz), 113.5 (d, $J_{C\text{-}F}$ = 23.6 Hz), 110.2, 105.1 (d, $J_{C\text{-}F}$ = 2.24 Hz), 76.4, 76.3, 76.2, 72.8, 70.1, 66.3, 50.3, 50.2, 49.6, 49.5, 45.7, 45.5, 45.2, 45.1, 44.8, 41.5, 39.3, 34.5, 30.7, 30.5, 29.3, 29.0, 28.5, 28.1, 27.9, 27.3, 27.2, 26.6, 26.5, 26.4, 23.9, 23.6, 23.4, 8.1; HRMS-ESI (m/z): $[M+H]^+$ calcd. for $C_{79}H_{96}FN_8O_{13}$: 1383.7075, found 1383.7064.

Desferridanoxamine-ciprofloxacin conjugate (3c)—tetra-*O*-Benzyl-trihydroxamate-*O*benzylciprofloxacin conjugate (**16**; 55.0 mg, 0.04 mmol) was dissolved in 6 mL of MeOH in an HCl-washed, 10 mL rb flask sealed under argon. The flask was charged with 10% Pd-C (15.0 mg) and exposed to a balloon of hydrogen gas (~1 atm). Reaction progress was monitored by RP-C18 TLC (1.5:1 CH_3CN:H_2O; $FeCl_3$ stain) and after 16 h there was no remaining starting material (**16**). The flask was flushed with argon and the mixture was diluted with MeOH, vacuum filtered through celite, and concentrated under reduced pressure. The resulting solid was dissolved in a minimal amount of MeOH and precipitated by addition of cold Et_2O. After trituration with Et_2O the desired product (**3c**) was obtained in 97% yield as a light yellow solid (36.1 mg, 0.039 mmol). Mp 94–96 °C (color change), 153–160 °C (dec.); ^{1}H-NMR (600 MHz, DMSO-d_6) δ 9.66 (br s, N-OH, 1 H), 9.62 (br s, N-OH, 2 H), 8.67 (s, 1 H), 7.93 (d, *J* = 13.2 Hz, 1 H), 7.78 (t, *J* = 4.4 Hz, 1 H), 7.58 (d, *J* = 7.3 Hz, 1 H), 4.35 (t, *J* = 5.0 Hz, 1 H), 4.04 (s, 1 H), 3.86–3.79 (m, 1 H), 3.74–3.66 (m, 4 H), 3.49–3.41 (m, 6 H), 3.39–3.34 (m, 4 H), 3.31–3.27 (m, 2 H), 3.03–2.95 (m, 4 H), 2.65 (t, *J* = 6.5 Hz, 2 H), 2.61–2.53 (m, 6 H), 2.30–2.21 (m, 4 H), 1.54–1.45 (m, 6 H), 1.43–1.34 (m, 6 H), 1.34–1.30 (m, 2 H), 1.27–1.16 (m, 8 H); ^{13}C-NMR (150 MHz, DMSO-d_6) δ 176.3, 172.0, 171.9, 171.9, 171.3, 171.2, 170.2, 165.9, 152.9 (d, $J_{C\text{-}F}$ = 249.1 Hz), 148.1, 144.9 (d, $J_{C\text{-}F}$ = 10.7 Hz), 139.1, 111.0 (d, $J_{C\text{-}F}$ = 23.0 Hz), 106.6, 60.6, 60.5, 49.6, 49.6, 49.2, 47.2, 47.1, 47.1, 44.4, 40.8, 38.4, 38.4, 38.3, 38.3, 35.9, 32.2, 32.1, 29.9, 29.8, 28.8, 27.6, 27.2, 26.9, 26.2, 26.1, 26.0, 23.5, 22.7, 7.6; HRMS-ESI (m/z): $[M+H]^+$ calcd. for $C_{44}H_{66}N_8O_{14}$: 933.4728, found 933.4744.

Determination of MIC Values by the Broth Microdilution Method

Antibacterial activity of the compounds was determined by measuring their minimum inhibitory concentrations (MICs) using the broth microdilution method according to the Clinical and Laboratory Standards Institute (CLSI, formerly the NCCLS) guidelines.(40) Each well of a 96-well microtiter plate was filled with 50 μL of sterile broth media (MHII, MHII – Fe, or MHII + Fe). Each test compound was dissolved in DMSO or H_2O making a 20 mM solution, then diluted with sterile MHII broth to 512 μM. Exactly 50 μL of the compound solution was added to the first well of the microtiter plate and 2-fold serial dilutions were made down each row of the plate. Exactly 50 μL of bacterial inoculum (5×10^5 CFU/mL) was then added to each well giving a total volume of 100 μL/well and a final compound concentration gradient of 128 μM. 0.0625 μM. The plate was incubated at 37 °C for 18 h and then each well was examined for bacterial growth. The MIC was recorded as the lowest compound concentration (μM) inhibiting visible bacterial growth as judged by turbidity of the culture media relative to a row of wells filled with a DMSO standard. Ciprofloxacin was included in a control row at a concentration gradient of 32 μM–0.0156 μM as well as a solvent control row.

For MIC studies using mixtures of compounds, both test compounds were diluted to 20 mM in DMSO as one homogeneous solution. The DMSO solution was then diluted with sterile broth media to give a solution at 512 μM for both compounds. Finally, 50 μL of the mixed compound broth solution was used in the assay exactly as described previously for single compound experiments.

General Procedure for the Agar Diffusion Paper Strip Siderophore-Sideromycin Competition Assay

A culture of *S. aureus* SG511 was grown in LB broth for 18–24 h and a standard cell suspension of 1.5×10^6 CFU/mL was prepared in saline solution (0.9% NaCl) according to a 0.5 $BaSO_4$ McFarland Standard.(60) The standardized cell suspension (0.1 mL) was added to 34 mL of sterile, melted MHII – Fe iron-deficient agar tempered to 47–50 °C. After gentle mixing, the inoculated agar media was poured into a sterile plastic petri dish (145 mm × 20 mm) and allowed to solidify near a flame with the lid cracked for ~30 min. Solutions of the test compounds dissolved in a 1:10 mixture of DMSO:MeOH (**3a, 3b**, and **3c**) or sterile, distilled, and deionized H_2O (**3a-Fe, DFO-B, FO-B**, Lorabid®, and ciprofloxacin) were prepared at the desired concentration (2.0 mM for **3a, 3a-Fe, 3b, DFO-B**, and **FO-B**; 0.5 mM for **3c**; 0.1 mM for Lorabid®; 5 μg/mL for ciprofloxacin). Sterile filter paper strips (Whatman No. 1 Standard Grade; cut to ~1 × 8 cm) were soaked in the test compound and laid on the surface of the inoculated agar media as shown in Figure 5. The petri dishes were incubated at 37 °C for 18–24 hours and photographed after 48 hours.

General Procedure for the Quantitative Agar Diffusion Antibiotic Susceptibility Assay

Antibacterial activity of the compounds was determined by a modified Kirby-Bauer agar diffusion assay.(46–47) Overnight cultures of test organisms were grown in LB broth for 18–24 h and standard cell suspensions of 1.5×10^6 CFU/mL were prepared in saline solution (0.9% NaCl) according to a 0.5 $BaSO_4$ McFarland Standard.(60) Each standardized cell suspension (0.1 mL) was added to 34 mL of sterile, melted agar (MHII, MHII – Fe, or MHII + Fe) tempered to 47.50 °C. After gentle mixing, the inoculated agar media was poured into a sterile plastic petri dish (145 mm × 20 mm) and allowed to solidify near a flame with the lid cracked for ~30 min. Wells of 9.0 mm diameter were cut from the petri dish agar and filled with exactly 50 μL of the test sample solution. For studies using mixtures of compounds, both test compounds were diluted to equal concentrations as one homogeneous solution and 50 μL of the mixed compound solution was added to the sample

well. The petri dish was incubated at 37 °C for 18.24 h and the inhibition zone diameters were measured (mm) with an electronic caliper after 24.48 h.

Supplementary Material

Refer to Web version on PubMed Central for supplementary material.

Acknowledgments

We gratefully acknowledge the use of NMR facilities provided by the Lizzadro Magnetic Resonance Research Center at The University of Notre Dame (UND) and the mass spectrometry services provided by The UND Mass Spectrometry & Proteomics Facility (Mrs. N. Sevova, Dr. W. Boggess, and Dr. M. V. Joyce; supported by the National Science Foundation under CHE-0741793). We thank Dr. Viktor Krch.ak (UND) for assistance with HPLC. We are grateful to Prof. Shariar Mobashery (UND) and Dr. Sergei Vakulenko (UND) for providing the *ESKAPEE* panel of bacteria and Dr. Nuno Tiago GiaoAntunes (UND) for determination of some preliminary MIC values against the panel. TAW gratefully acknowledges The UND Chemistry-Biochemistry-Biology (CBBI) Interface Program funded by the NIH (T32GM075762) for three years of fellowship support and funding an internship at the Hans Knoll Institute (HKI) in Jena, Germany to learn microbiological assays. TAW sincerely thanks the HKI for hosting such an internship. TAW also thanks the UND Department of Chemistry and Biochemistry (Grace Fellowship), the UND Center for Environmental Science and Technology (CEST), and Bayer for additional fellowship support. We acknowledge The University of Notre Dame and the NIH for financial support of this work.

Abbreviations

ABC	ATP-binding cassette transporter
acac	acetylacetonate
ATCC	American Type Culture Collection
Bn	benzyl
Boc	*tert*-butoxycarbonyl
CFU	colony forming unit
DFO-B	desferrioxamine B
DMAP	4-dimethylaminopyridine
DMF	dimethylformamide
DMSO	dimethylsulfoxide
ESI	electrospray ionization
ExbB/D	inner membrane bound protein of TonB complex
FO-B	ferrioxamine B
Fur	ferric uptake regulator protein
HPLC	high-performance liquid chromatography
HRMS	high-resolution mass spectrometry
MHII	Mueller–Hinton media no. II
MIC	minimum inhibitory concentration
NMR	nuclear magnetic resonance
OMR	outer membrane receptor protein
OMT	TonB-dependent outer membrane siderophore transport protein

PNB	*para*-nitrobenzyl
Red	iron reductase enzyme
SPBP	siderophore periplasmic binding protein
TFA	trifluoroacetic acid
TLC	thin layer chromatography
TonB	membrane-spanning protein complex involved in siderophore transport

References

1. Boucher HW, Talbot GH, Bradley JS, Edwards JE Jr, Gilbert D, Rice LB, Scheld M, Spellberg B, Bartlett J. Bad bugs, no drugs: No ESKAPE! An update from the Infectious Diseases Society of America. Clin. Infect. Dis. 2009; 48:1–12. [PubMed: 19035777]
2. Fischback MA, Walsh CT. Antibiotics for emerging pathogens. Science. 2009; 325:1089–1093. [PubMed: 19713519]
3. Payne DJ, Gwynn MN, Holmes DJ, Pompliano DL. Drugs for bad bugs: Confronting the challenges of antibacterial discovery. Nat. Rev. Drug Discov. 2007; 6:29–40. [PubMed: 17159923]
4. Pereira MP, Kelley SO. Maximizing the therapeutic window of an antimicrobial drug by imparting mitochondrial sequestration in human cells. J. Am. Chem. Soc. 2011; 133:3260–3263. [PubMed: 21322645]
5. Silver LL. Are natural products still the best source for antibacterial discovery? The bacterial entry factor. Expert Opin. Drug Discov. 2008; 3:487–500. [PubMed: 23484922]
6. O'Shea R, Moser HE. Physiochemical properties of antibacterial compounds: Implications in drug discovery. J. Med. Chem. 2008; 51:2871–2878. [PubMed: 18260614]
7. Ranny DF. Biomimetic transport and rational drug delivery. Biochem. Pharmacol. 2000; 59:105–114. [PubMed: 10810444]
8. Christofferson RE. Antibiotics: An investment worth making? Nat. Biotechnol. 2006; 24:1512–1514. [PubMed: 17160052]
9. Braun V, Endriß F. Energy-coupled outer membrane transport proteins and regulatory proteins. Biometals. 2007; 20:219–231. [PubMed: 17370038]
10. Ji C, Juarez-Hernandez RE, Miller MJ. Exploiting bacterial iron acquisition: siderophore conjugates. Future Med. Chem. 2012; 4:297–313. [PubMed: 22393938]
11. Roosenberg JM, Lin Y-M, Lu Y, Miller MJ. Studies and syntheses of siderophores, microbial iron chelators, and analogs as potential drug delivery agents. Curr. Med. Chem. 2000; 7:159–197. [PubMed: 10637361]
12. Frederick RE, Mayfield JA, DuBois JL. Iron trafficking as an antimicrobial target. Biometals. 2009; 22:583–593. [PubMed: 19350396]
13. Miethke M, Marahiel MA. Siderophore-based iron acquisition and pathogen control. Microbiol. Mol. Biol. Rev. 2007; 71:413–451. [PubMed: 17804665]
14. Hider RC, Kong X. Chemistry and biology of siderophores. Nat. Prod. Rep. 2010; 27:637–657. [PubMed: 20376388]
15. Wandersman C, Delepelaire P. Bacterial iron sources: From siderophores to hemophores. Ann. Rev. Microbiol. 2004; 58:611–647. [PubMed: 15487950]
16. Challis GL, Hopwood DA. Synergy and contingency as driving forces for the evolution of multiple secondary metabolite production by *Streptomyces* species. Proc. Natl. Acad. Sci. U.S.A. 2003; 100:14555–14561. [PubMed: 12970466]
17. Braun V, Pramanik A, Gwinner T, Koberle M, Bohn E. Sideromycins: Tools and antibiotics. Biometals. 2009; 22:3–13. [PubMed: 19130258]
18. Reynolds DM, Schatz A, Waksman SA. Grisein, a new antibiotic produced by a strain of *Streptomyces griseus*. Proc. Soc. Exp. Biol. Med. 1947; 64:50–54. [PubMed: 20285459]

19. Benz G, Schroder T, Kurz J, Wunsche C, Karl W, Steffens G, Pfitzner J, Schmidt D. Konstitution der deferriform der albomycine δ_1, δ_2, und ε. Angew. Chem. Int. Ed. Engl. 1982; 21:527–528.
20. Ferguson AD, Braun V, Fiedler HP, Coulton JW, Diedrichs K, Welte W. Crystal structure of the antibiotic albomycin in complex with the outer membrane transporter FhuA. Protein Sci. 2000; 9:956–963. [PubMed: 10850805]
21. Clarke TE, Braun V, Winkelmann G, Tari LW, Vogel HJ. X-ray crystallographic structures of the *Escherichia coli* periplasmic protein FhuD bound to hydroxamate-type siderophores and the antibiotic albomycin. J. Biol. Chem. 2002; 277:13966–13972. [PubMed: 11805094]
22. Braun V, Gunthner K, Hantke K, Zimmermann L. Intracellular activation of albomycin in *Escherichia coli* and *Salmonella typhimurium*. J. Bacteriol. 1983; 156:308–315. [PubMed: 6352681]
23. Zeng Y, Kulkarni A, Yang Z, Patil PB, Zhou W, Chi X, Van Lanen S, Chen S. Biosynthesis of albomycin δ_2 provides a template for assembling siderophore and aminoacyl-tRNA synthetase inhibitor conjugates. ACS Chem. Biol. 2012; 7:1565–1575. [PubMed: 22704654]
24. Vertesy L, Aretz W, Fehlhaber H-W, Koger H. Salmycin A-D, antibiotika aus *Streptomyces violaceus* DSM 8286, mit siderophore-aminoglycosidstruktur. Helv. Chim. Acta. 1995; 78:46–60.
25. Dong L, Roosenberg JM, Miller MJ. Total synthesis of desferrisalmycin B. J. Am. Chem. Soc. 2002; 124:15001–15005. [PubMed: 12475343]
26. Bunet R, Brock A, Rexer H-U, Takano E. Identification of genes involved in siderophore transport in *Streptomyces coelicolor* A3(2). FEMS Microbiol. Lett. 2006; 262:57–64. [PubMed: 16907739]
27. Wencewicz TA, Mollmann U, Long TE, Miller MJ. Is drug release necessary for antimicrobial activity of siderophore-drug conjugates? Syntheses and biological studies of the naturally occurring salmycin "Trojan Horse" antibiotics and synthetic desferridanoxamine-antibiotic conjugates. Biometals. 2009; 22
28. Walsh, C. Antibiotics: Actions, origins, and resistance. Washington, D.C.: ASM Press; 2003.
29. Roosenberg JM Jr, Miller MJ. Total synthesis of the siderophore danoxamine. J. Org. Chem. 2000; 65:4833–4838. [PubMed: 10956460]
30. Wencewicz TA, Oliver AG, Miller MJ. Iron(III)-templated macrolactonization of trihydroxamate siderophores. Org. Lett. 2012; 14:4390–4393. [PubMed: 22906163]
31. Jung ME, Yang EC, Vu BT, Kiankarimi M, Spyrou E, Kaunitz J. Glycosylation of fluoroquinolones through direct oxygenated polymethylene linkages as a sugar-mediated active transport system for antimicrobials. J. Med. Chem. 1999; 42:3899–3909. [PubMed: 10508438]
32. Testero, SA.; Fisher, JF.; Mobashery, S. β-Lactam antibiotics. In: Abraham, DJ.; Rotella, DP., editors. Burger's Medicinal Chemistry, Drug Discovery and Development. 7 ed. Hoboken: Wiley; 2010. p. 259-404.
33. Mitscher LA. Bacterial topoisomerase inhibitors: Quinolone and pyridone antibacterial agents. Chem. Rev. 2005; 105:559–592. [PubMed: 15700957]
34. Brochu A, Brochu N, Nicas TI, Parr TR Jr, Minnick AA Jr, Dolence EK, McKee JA, Miller MJ, Lavoie MC, Malouin F. Modes of action and inhibitory activities of new siderophore-β-lactam conjugates that use specific iron uptake pathways for entry into bacteria. Antimcrob. Agents Chemother. 1992; 36:2166–2175.
35. Hennard C, Truong QC, Desnottes J-F, Paris J-M, Moreau NJ, Abdallah MA. Synthesis and activities of pyoverdin-quinolone adducts: A prospective approach to a specific therapy against *Pseudomonas aeruginosa*. J. Med. Chem. 2001; 44:2139–2151. [PubMed: 11405651]
36. Ghosh A, Ghosh M, Niu C, Malouin F, Moellmann U, Miller MJ. Iron transport-mediated drug delivery using mixed-ligand siderophore-β-lactam conjugates. Chem. Biol. 1996; 3:1011–1019. [PubMed: 9000006]
37. McKee JA, Sharma SK, Miller MJ. Iron transport mediated drug delivery systems: Synthesis and antibacterial activity of spermidine- and lysine-based siderophore-β-lactam conjugates. Bioconjugate Chem. 1991; 2:281–291.
38. Ghosh A, Miller MJ. Synthesis of novel citrate-based siderophores and siderophore-β-lactam conjugates. J. Org. Chem. 1993; 58:7652–7659.

39. Ghosh M, Miller MJ. Iron transport-mediated drug delivery: Synthesis and biological evaluation of cyanuric acid-based siderophore analogs and β-lactam conjugates. J. Org. Chem. 1994; 59:1020–1026.
40. CLSI. Methods for dilution antimicrobial susceptibility tests for bacteria that grow aerobically. 8th ed. Villanova, PA: 2009.
41. de Lorenzo, V.; Perez-Martin, J.; Escolar, L.; Pesole, G.; Bertoni, G. Mode of binding of the Fur protein to target DNA: Negative regulation of iron-controlled gene expression. In: Crosa, JH.; Mey, AR.; Payne, SM., editors. Iron Transport in Bacteria. Washington, D.C.: ASM Press; 2004. p. 185-196.
42. Mollmann U, Heinisch L, Bauernfeind A, Kohler T, Ankel-Fuchs D. Siderophores as drug delivery agents: Application of the "Trojan Horse" strategy. Biometals. 2009; 22:615–624. [PubMed: 19214755]
43. Heinisch L, Wittmann S, Stoiber T, Berg A, Ankel-Fuchs D, Mollmann U. Highly antibacterial active aminoacyl penicillin conjugates with bis-catecholate siderophores based on secondary diamino acids and related compounds. J. Med. Chem. 2002; 45:3032–3040. [PubMed: 12086488]
44. Pramanik A, Braun V. Albomycin uptake via a ferric hydroxamate transport system of *Streptococcus pneumoniae* R6. J. Bacteriol. 2006; 188:3878–3886. [PubMed: 16707680]
45. Reniere, ML.; Pishchany, G.; Skaar, EP. Iron uptake in *Staphylococci*. In: Cornelis, P.; Andrews, SC., editors. Iron uptake and homeostasis in microorganisms. Norfolk: Caister Academic Press; 2010. p. 247-264.
46. Wencewicz TA, Yang B, Rudloff JR, Oliver AG, Miller MJ. N-O Chemistry for antibiotics: Discovery of *N*-alkyl-*N*-(pyridin-2-yl)hydroxylamine scaffolds as selective antibacterial agents using nitroso Diels-Alder and ene chemistry. J. Med. Chem. 2011; 54:6843–6858. [PubMed: 21859126]
47. Bauer AW, Kirby WMM, Sherris JC, Turck M. Antibiotic susceptibility testing by a standardized single disk method. Am. J. Clin. Pathol. 1966; 45:493–496. [PubMed: 5325707]
48. Krewulak KD, Vogel HJ. Structural biology of bacterial iron uptake. Biochim. Biophys. Acta. 2008; 1778:1781–1804. [PubMed: 17916327]
49. Krewulak, KD.; Peacock, RS.; Vogel, HJ. Periplasmic binding proteins involved in bacterial iron uptake. In: Cornelis, P.; Andrews, SC., editors. Iron uptake and homeostasis in microorganisms. Norfolk: Caister Academic Press; 2010. p. 113-129.
50. Ji C, Miller MJ. Chemical syntheses and in vitro antibacterial activity of two desferrioxamine B-ciprofloxacin conjugates with potential esterase and phosphatase triggered drug release linkers. Bioorg. Med. Chem. 2012; 20:3828–3836. [PubMed: 22608921]
51. De Sarro A, De Sarro G. Adverse reactions to fluoroquinolones: An overview on mechanistic aspects. Curr. Med. Chem. 2001; 8:371–384. [PubMed: 11172695]
52. Kontoghiorghes GJ, Eracleous E, Economides C, Kolnagou A. Advances in iron overload therapies. Prospects for effective use of deferipron (L1), deferoxamine, the new experimental chelators ICL670, GT56-252, L1NAII and their combinations. Curr. Med. Chem. 2005; 12:2663–2681. [PubMed: 16305464]
53. Vertesy, L.; Aretz, W.; Fehlhaber, H-W.; Ganguli, BN. Salmycins, a process for their preparation and their use as a pharmaceutical. U.S. Patent. 5475094. 1995 Dec 12.
54. Vertesy, L.; Werner, A.; Fehlhaber, H-W. Chelating agents, their preparation from the antibiotics salmycin A, B, C, or D, and their use. U.S. Patent. 5519123. 1996 May 21.
55. Clifton MC, Corrent C, Strong RK. Siderocalins: Siderophore-binding proteins of the innate immune system. Biometals. 2009; 22:557–564. [PubMed: 19184458]
56. Barza M. Challenges to antibiotic activity in tissues. Clin. Infect. Dis. 1994; 19:910–915. [PubMed: 7893878]
57. Imbuluzqueta E, Gamazo C, Ariza J, Blanco-Prieto MJ. Drug delivery systems for potential treatment of intracellular bacterial infections. Front. Biosci. 2010; 15:397–417. [PubMed: 20036827]
58. Heo J, Hua SZ. An overview of recent strategies in pathogen sensing. Sensors. 2009; 9:4483–4502. [PubMed: 22408537]

59. Zheng T, Nolan EM. Siderophore-based detection of Fe(III) and microbial pathogens. Metallomics. 2012; 4:866–880. [PubMed: 22854844]

60. Murray, PR.; Baron, EJ.; Pfaller, MA.; Tenover, FC.; Yolken, RH. Manual of clinical microbiology. 7 ed. Washington, D.C.: American Society for Microbiology; 1999.

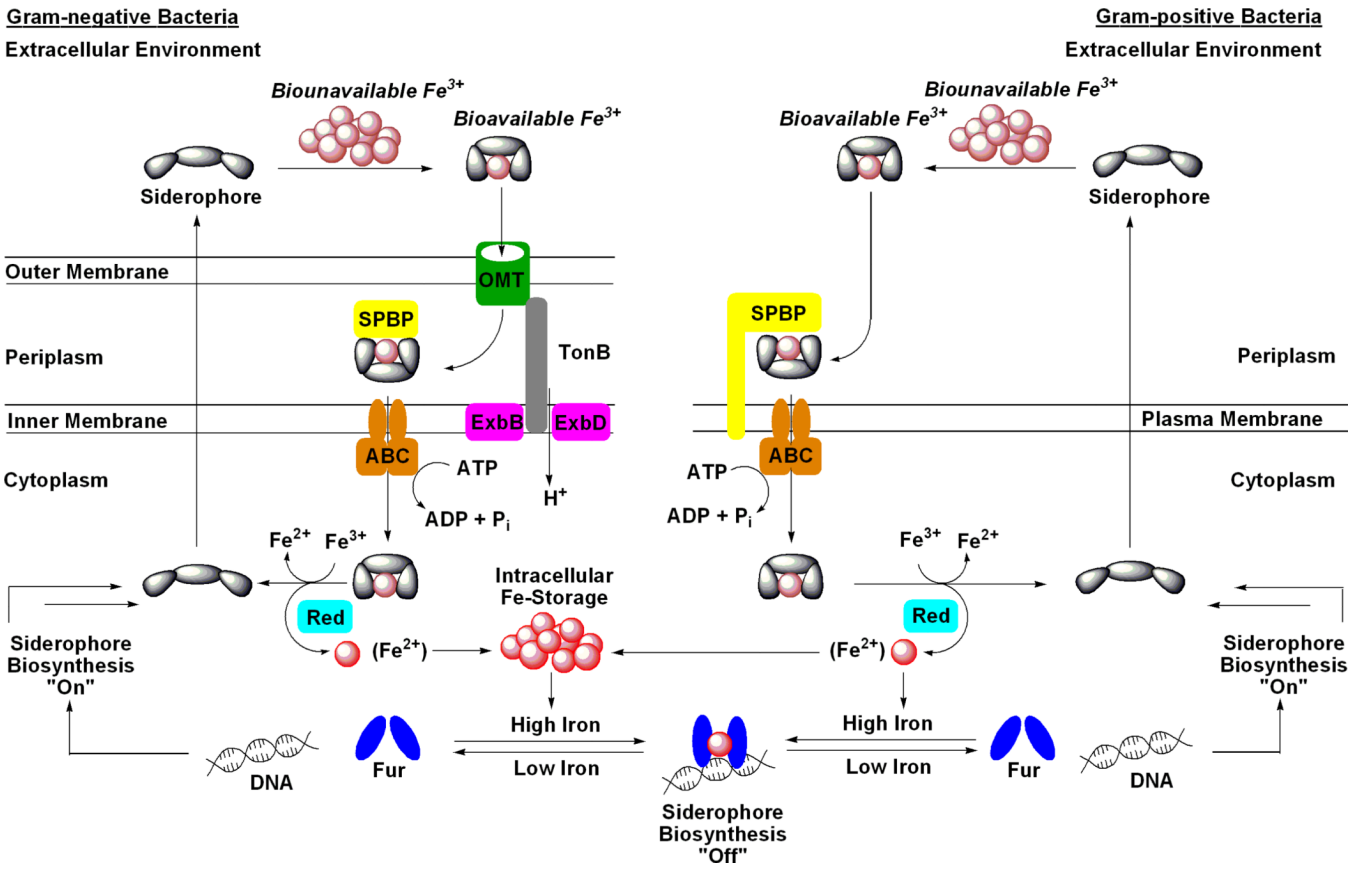

Figure 1.

Generic schematic of siderophore-mediated iron uptake and genetic regulation in Gram-negative and Gram-positive bacteria. Iron metabolism in bacteria is under genetic control by the ferric uptake regulator (Fur) transcription factor protein. During times of iron abundance, the Fur protein complexes Fe(II) and adopts a conformation that binds to a region of DNA known as a ‘Fur box’ which represses the expression of siderophore-related proteins, including biosynthetic enzymes. During times of iron deficiency, the apo-Fur protein dissociates from the ‘Fur box’ allowing expression of siderophore-related genes. The siderophore system is now fully functional and begins with siderophore biosynthesis and efflux to the extracellular environment. For Gram-negative bacteria, after the siderophore chelates Fe(III) to form a soluble complex it is transported into the periplasm by a high affinity outer membrane transport protein (OMT; formerly called OMR). This transport is driven by the proton motive force with energy transfer mediated by the membrane-spanning TonB-ExbB/D protein complex. The Fe(III)-loaded siderophore is then bound by a siderophore periplasmic binding protein (SPBP) and trafficked to an ATP-binding cassette transporter (ABC) that moves the siderophore-Fe(III) complex into the cytoplasm. The iron nutrient is then removed from the siderophore, typically via reduction of Fe(III) to Fe(II) by an iron reductase enzyme (Red), and is distributed to parts of the cell in need or stored in bacterioferritin. In most cases, the siderophore is then recycled for further use. Gram-positive bacteria lack the outer membrane found in Gram-negative bacteria and therefore also lack the OMTs and TonB complex. Instead, extracellular siderophore-Fe(III) complexes are recognized and transported by membrane-anchored SPBPs. The remaining steps of the siderophore pathway in Gram-positive bacteria are analogous to those described for Gramnegative bacteria. This figure was inspired by a variety of siderophore transport

diagrams reported in the literature which also describe these pathways in great detail.(13–15)

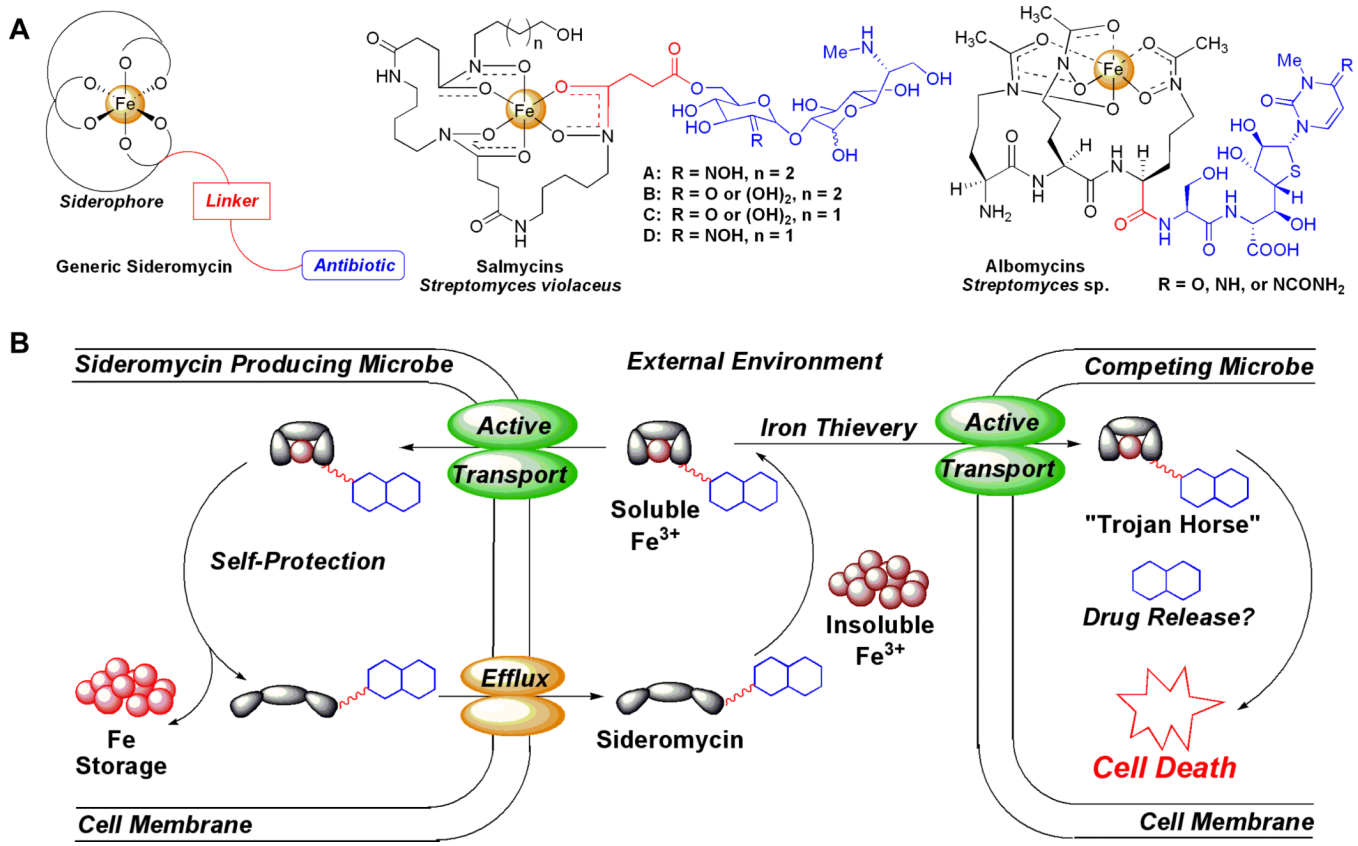

Figure 2.

(A) Structures of generic and natural sideromycins (albomycins and salmycins). (B) Generic schematic of sideromycins as 'Trojan Horse' antibiotic delivery agents. Sideromycins (siderophore-antibiotic conjugates) act as normal siderophores for sideromycin producing microbes, which can self-protect from the antibiotic, by scavenging extracellular Fe(III) via the pathways described in figure 1. For competing microbes attempting to steal the sideromycinbound Fe(III) nutrient, active transport of the sideromycin via siderophore uptake pathways exposes the competing microbe to the antibiotic, for which it lacks the inherent resistance found in the producer, and ultimately causes cell death.

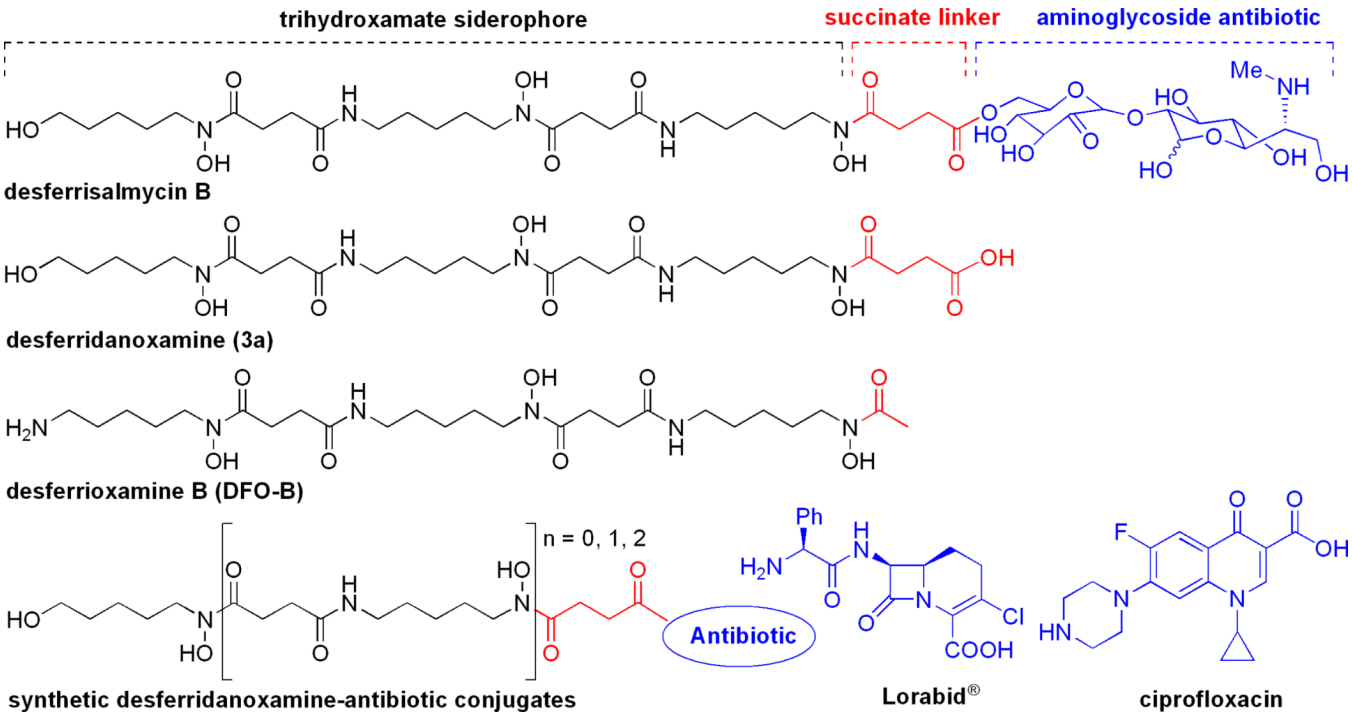

Figure 3.

Structures of desferrisalmycin B, desferridanoxamine (**3a**), desferrioxamine B (**DFO-B**), and synthetic desferridanoxamine-antibiotic conjugates from this study.

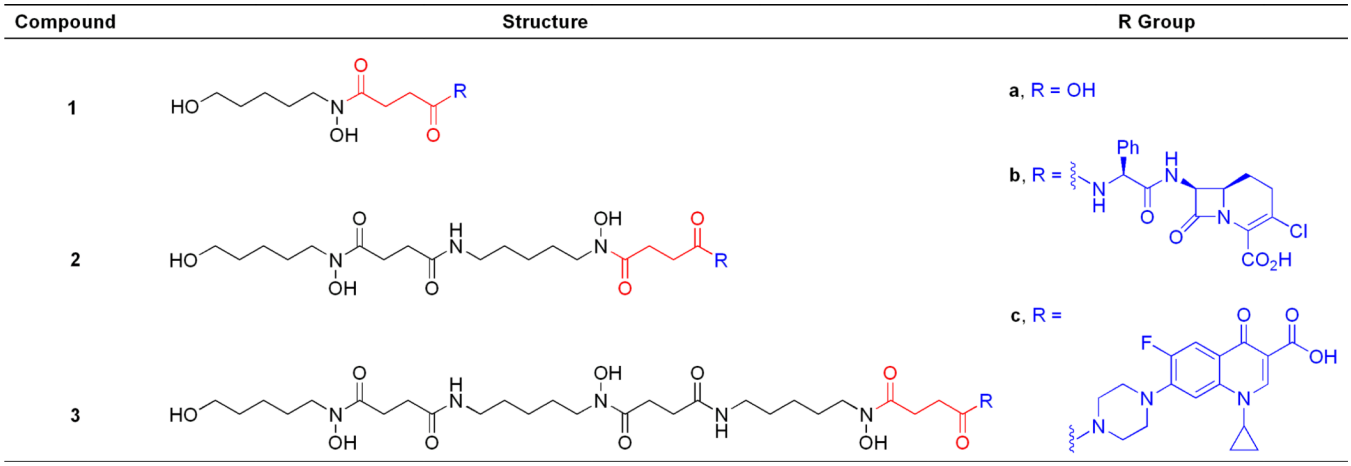

Figure 4.
Structures of synthetic hydroxamate siderophores (**1a–3a**) and sideromycins (**1b–3b** and **1c–3c**) used in this work.

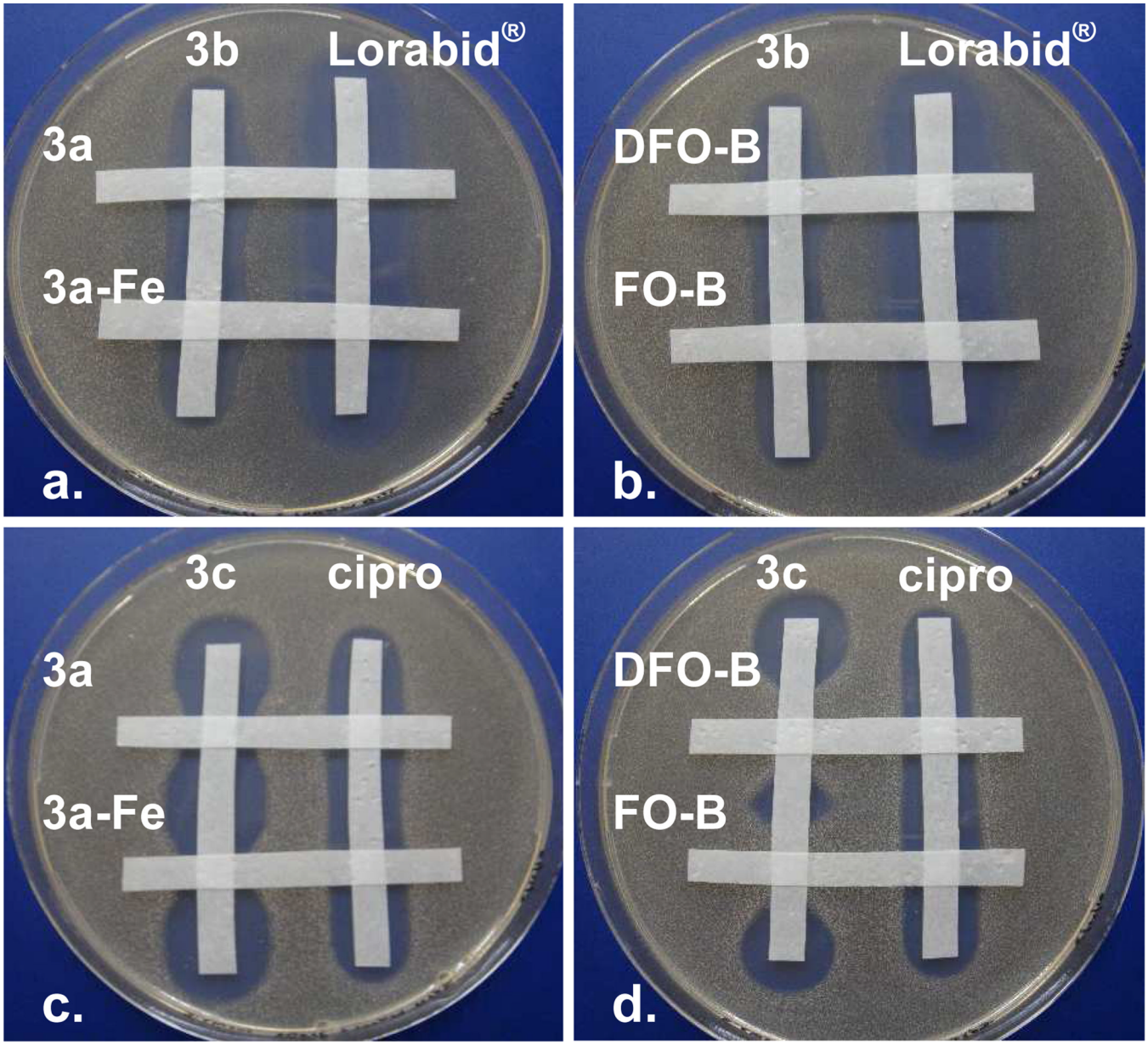

Figure 5.

Agar diffusion competition assay for conjugates **3b** and **3c** and siderophores **3a, 3a-Fe, DFO-B**, and **FO-B** tested against *S. aureus* SG511. Siderophores **3a, 3a-Fe, DFO-B**, and **FO-B** clearly antagonize the anti-*S. aureus* activity of the fluoroquinolone conjugate **3c** (c,d), but not the β-lactam conjugate **3b** (a, b). Images are not to actual scale.

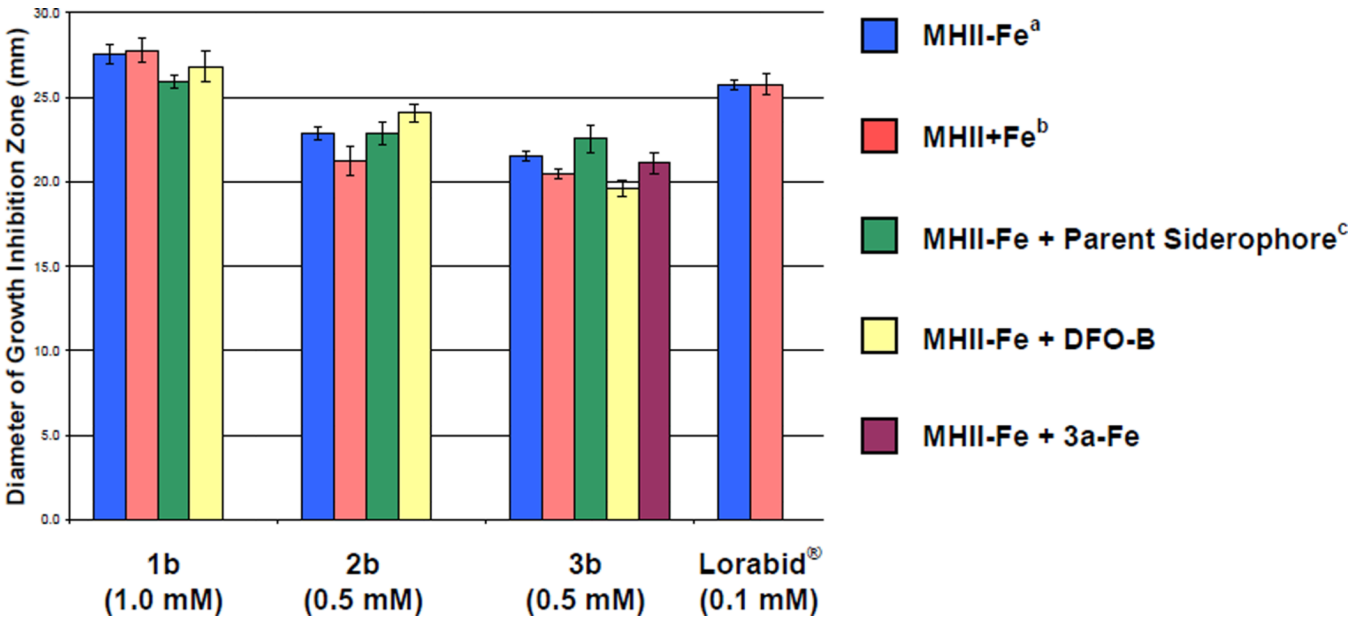

Figure 6.

Effect of varying Fe(III) concentrations and presence of competing siderophores (**1a, 2a, 3a, 3a-Fe, DFO-B**) on the antibacterial activity of β-lactam sideromycins (**1b, 2b**, and **3b**) against *S. aureus* SG511 in the agar diffusion assay. The vertical axis indicates the diameter of the growth inhibition zone in mm and horizontal axis represents the test compound. The assay was performed in triplicate and standard deviations are indicated by error bars. [a]MHII-Fe: Mueller-Hinton agar No. 2 + 100 μM 2,2'-bipyridine. [b]MHII+Fe: Mueller-Hinton agar No. 2 + 100 μM $FeCl_3$. [c]Parent siderophore refers to the iron-free siderophore (**1a, 2a**, and **3a**) with the same compound numeral as the corresponding sideromycin (**1b, 2b**, and **3b**, respectively). Data for all mixtures corresponds to a 1:1 molar ratio of test compounds. 50 μL of sample at the concentration indicated in parentheses under the compound numbers were added to 9 mm wells as described in the experimental section. The tabulated numerical data for this chart is provided in the Supporting Information (Tables S2 and S3).

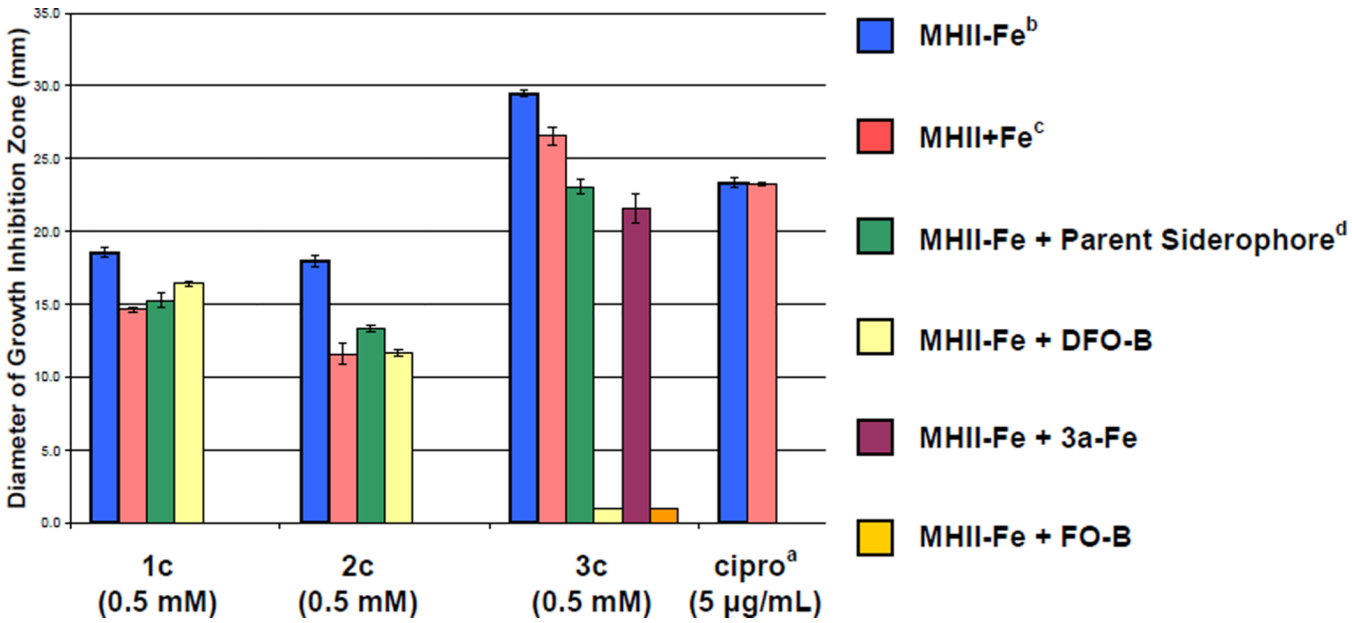

Figure 7.

Effect of varying Fe(III) concentrations and presence of competing siderophores (**1a, 2a, 3a, 3a-Fe, DFO-B**, and **FO-B**) on the antibacterial activity of fluoroquinolone sideromycins (**1c, 2c**, and **3c**) against *S. aureus* SG511 in the agar diffusion assay. The vertical axis indicates the diameter of the growth inhibition zone in mm and the horizontal axis indicates the test compound. The assay was performed in triplicate. [a]Ciprofloxacin was used as a control. [b]MHII-Fe: Mueller-Hinton agar No. 2 + 100 µM 2,2'-bipyridine. [c]MHII+Fe: Mueller-Hinton agar No. 2 + 100 µM $FeCl_3$. [d]Parent siderophore refers to the iron-free siderophore (**1a, 2a**, and **3a**) with the same compound numeral as the corresponding sideromycin (**1c, 2c**, and **3c**, respectively). Data for all mixtures corresponds to a 1:1 molar ratio of test compounds. 50 µL of sample at the concentration indicated in parentheses under the compound numbers were added to 9 mm wells as described in the experimental section. The tabulated numerical data for this chart is provided in the Supporting Information (Tables S2 and S3).

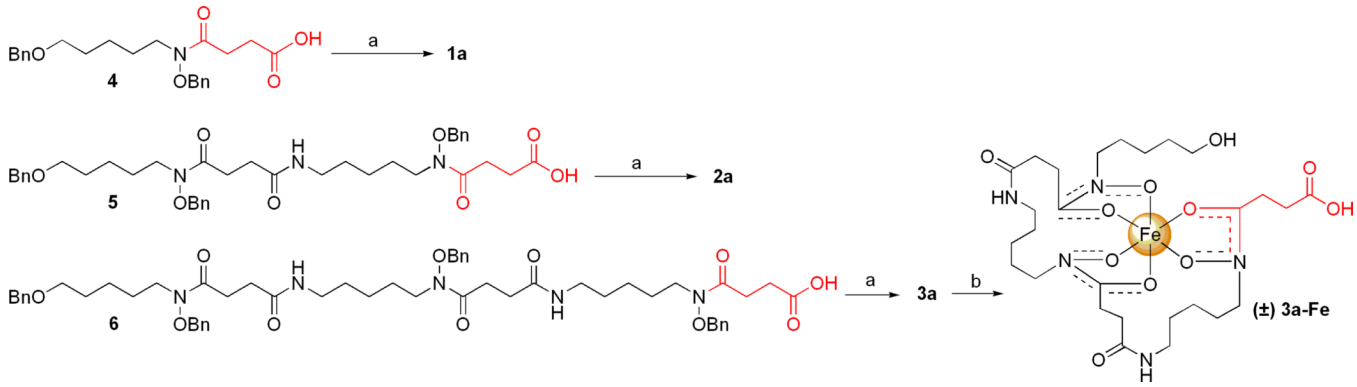

Scheme 1.

Syntheses of iron-free (**1a–3a**) and iron-bound (**3a-Fe**) hydroxamate siderophores.a

[a]Reagents and conditions: (a) 10% Pd-C, H_2 (1 atm), MeOH; 6 h, 88% for **1a**; 4.5 h, 90% for **2a**; 11 h, 86% for **3a**. (b) $Fe(acac)_3$, MeOH; 4 h, 99% for **3a-Fe**.

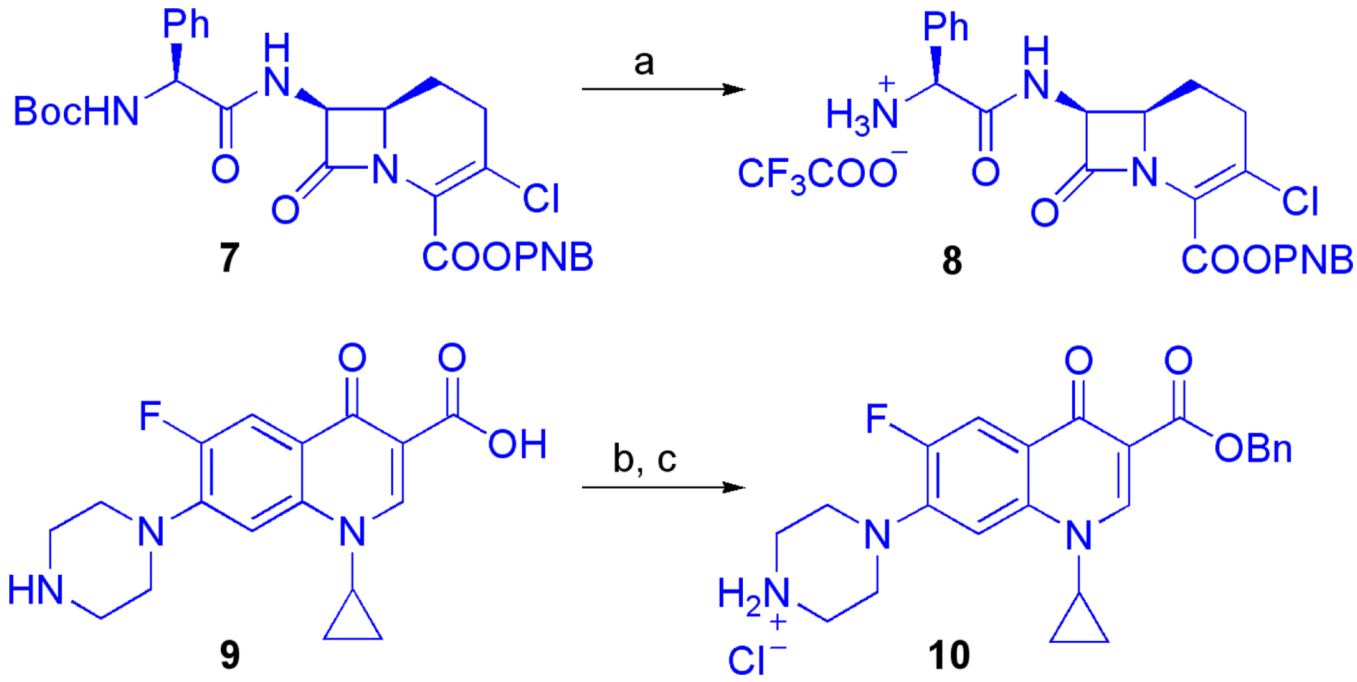

Scheme 2.

Synthesis of protected antibiotics (**8** and **10**) suitable for siderophore conjugation.a

[a]Reagents and conditions: (a) *N*-Boc-*O*-PNB-Lorabid® (**7**), TFA, CH_2Cl_2, 30 min, 99%. (b) ciprofloxacin (**9**), Boc_2O, $NaHCO_3$, DMF, 2.5h; then, BnBr, 90 °C, 25.5 h, 98%. (c) con. HCl, CH_2Cl_2, 40 min, 92%.

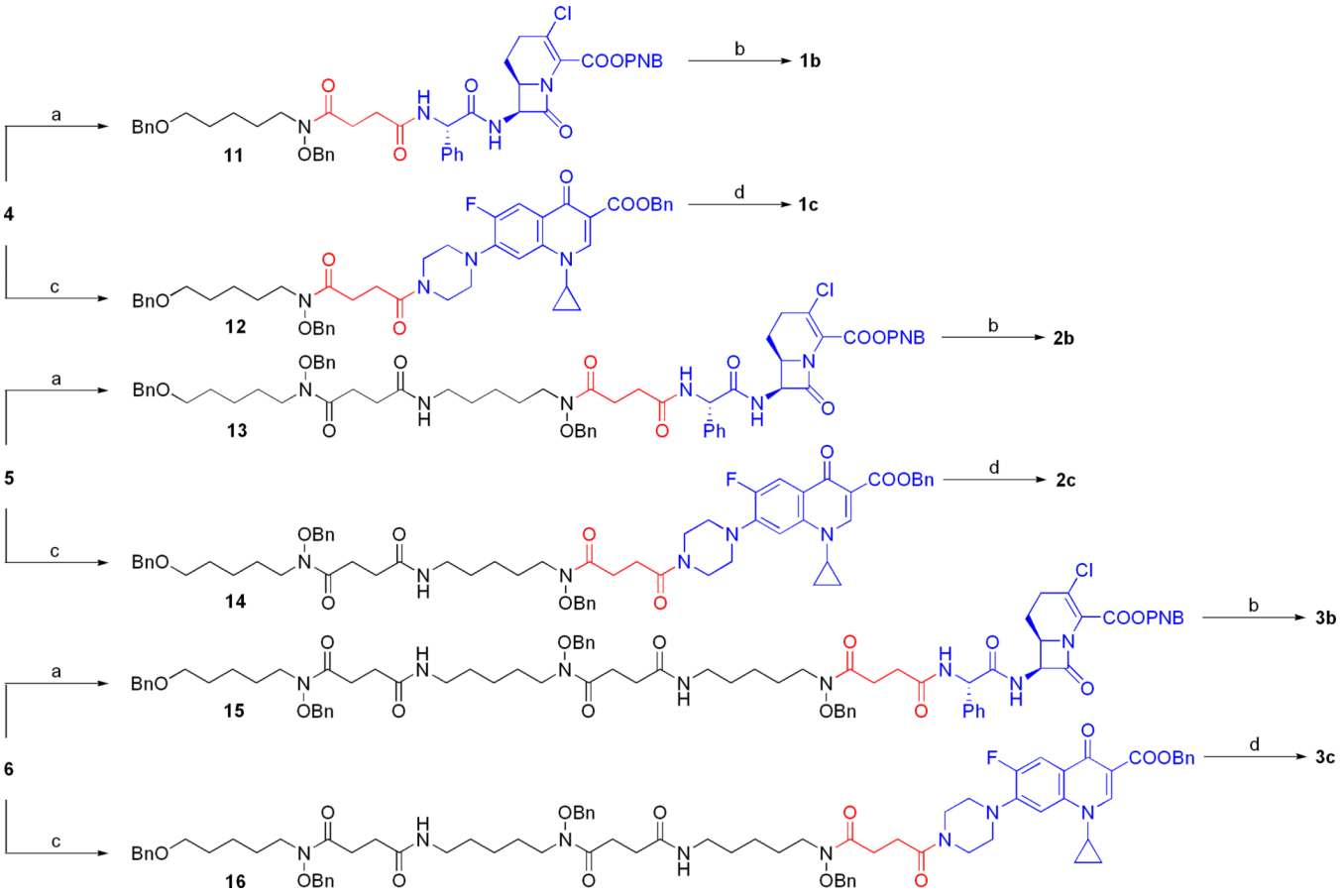

Scheme 3. Syntheses of hydroxamate sideromycins (1b–3b and 1c–3c).a

[a]Reagents and conditions: (a) **8**, *i*Pr$_2$EtN, DMAP, CH_2Cl_2; 18 h, 73% for **11**; 16 h, 66% for **13**; 20 h, 87% for **15**. (b) 10% Pd-C, H_2 (1 atm), HCl (3 equiv), DMF:H_2O (95:5); 41 h, 38% for **1b**; 24 h, 42% for **2b**; 24 h, 42% for **3b**. (c) **10**, *i*Pr$_2$EtN, DMAP, CH_2Cl_2; 5 h, 92% for **12**; 23 h, 66% for **14**; 4.5 h, 84% for **16**. (d) 10% Pd-C, H_2 (1 atm), MeOH; 12 h, 70% for **1c**; 16 h, 86% for **2c**; 16 h, 97% for **3c**.

Table 1

MIC values of compounds **1b–3b** and **1c–3c** against *ESKAPEE* panel of bacteria.[a,b]

Entry	Compound	Test Organisms						
		***E. faecium* NCTC 7171**	***S. aureus* SG 511**	***K. pneumonia* ATCC 700603**	***A. baumannii* ATCC 17961**	***P. aeruginosa* ATCC 27853**	***E. aerogenes* ATCC 35029**	***E. coli* ATCC 25922**
1	**1a**	>128	>128	>128	>128	>128	>128	>128
2	**2a**	>128	>128	>128	>128	>128	>128	>128
3	**3a**	>128	>128	>128	>128	>128	>128	>128
4	**3a–Fe**	>128	>128	>128	>128	128	>128	>128
5	**1b**	>128	16	>128	≥128	>128	>128	>128
6	**2b**	>128	64	>128	32	>128	>128	≥128
7	**3b**	>128	64	>128	64	>128	>128	128
8	**1c**	>128	32	16	16	128	4	2
9	**2c**	>128	64	128	64	64	4	2
10	**3c**	64	1	>128	≥128	>128	64	>128
11	Lorabid®	32	1	128	>128	>128	>128	2
12	ciprofloxacin	8	0.5	0.25	0.25	0.125	<0.015	<0.015

[a]MIC values were determined using the broth microdilution method in Mueller-Hinton broth No. 2 (MHII) using visual end point analysis according to the CLSI guidelines.(40)

[b]Each compound was tested in triplicate.

Table 2

MIC values (μM) of compounds **1b–3b** and **1c–3c** against *S. aureus* SG511 under varying concentrations of Fe(III).[a,b]

		Test Organism	
		Staphylococcus aureus SG511	
Entry	Compound	MHII + Fe[b]	MHII − Fe[c]
1	**1b**	16	16
2	**2b**	128	64
3	**3b**	128	64
4	**1c**	64	32
5	**2c**	64	64
6	**3c**	4	1
8	Lorabid®	1	1
9	ciprofloxacin	0.5	0.5

[a] MIC values were determined using the broth microdilution method using visual end point analysis according to the CLSI guidelines.(40)

[b] Each compound was tested in triplicate.

[c] MHII + Fe: Mueller-Hinton Broth No. 2 + 100 μM $FeCl_3$.

[d] MHII − Fe: Mueller-Hinton Broth No. 2 + 100 μM 2,2'-bipyridine.

Table 3

MIC values (μM) of compounds **1b–3b** and **1c–3c** against *S. aureus* SG511 in the presence of competing siderophores.[a,b,c]

		Test Organism
		***Staphylococcus aureus* SG511**
Entry	**Compound[d]**	**MHII − Fe[e]**
1	**1b + 1a**	16
2	**1b + DFO-B**	16
3	**2b + 2a**	32
4	**2b + DFO-B**	16
5	**3b + 3a**	32
6	**3b + 3a-Fe**	64
7	**3b + DFO-B**	32
8	**3b + FO-B**	64
9	**1c + 1a**	32
10	**1c + DFO-B**	16
11	**2c + 2a**	64
12	**2c + DFO-B**	64
13	**3c + 3a**	1
14	**3c + 3a-Fe**	1
15	**3c + DFO-B**	128
16	**3c + FO-B**	>128

[a] MIC values were determined using the broth microdilution method using visual end point analysis according to the CLSI guidelines.(40)

[b] Each compound was tested in triplicate.

[c] Data presented here should be compared to MIC values in Table 1 for compounds **1b–3b** and **1c– 3c**.

[d] Compounds were tested as 1:1 molar mixtures.

[e] MHII – Fe: Mueller-Hinton Broth No. 2 + 100 μM 2,2'-bipyridine